



**Joana Gonzalez Loureiro**

Licenciada em Conservação e Restauro

**Archaeometallurgical study of the Proto-historic  
collection of Moinhos de Golas (North Portugal):  
A forecast for technological changes?**

Dissertação para obtenção do Grau de Mestre em  
Conservação e Restauro

Orientador: Doutora Elin Maria Soares de Figueiredo  
Co-orientador: Professor Doutor Rui Jorge Cordeiro Silva  
Co-orientador: Professora Doutora Maria de Fátima Araújo

Júri:

Presidente: Professora Doutora Maria João Seixas de Melo  
Arguente: Professor Doutor António Manuel Monge Soares  
Vogal: Doutora Elin Maria Soares de Figueiredo



FACULDADE DE  
CIÊNCIAS E TECNOLOGIA  
UNIVERSIDADE NOVA DE LISBOA

**Dezembro 2014**

**Joana Gonzalez Loureiro**

Department of Conservation and Restoration  
Master degree in Conservation and Restoration

**Archaeometallurgical study of the Proto-historic collection  
of Moinhos de Golas (North Portugal):  
A forecast for technological changes?**

Dissertation presented at Faculdade de Ciências e Tecnologia, Universidade  
Nova de Lisboa, in performance of the requirements for the Master degree in  
Conservation and Restoration

Supervisor: Elin Figueiredo  
Co-supervisor: Rui J.C. Silva  
Co-supervisor: Maria de Fátima Araújo

**December 2014**

*Archaeometallurgical study of the Proto-historic collection of Moinhos de Golas (North Portugal): A forecast for technological changes? ©*

A Faculdade de Ciências e Tecnologia e a Universidade Nova de Lisboa têm o direito, perpétuo e sem limites geográficos, de arquivar e publicar esta dissertação através de exemplares impressos reproduzidos em papel ou de forma digital, ou por qualquer outro meio conhecido ou que venha a ser inventado, e de a divulgar através de repositórios científicos e de admitir a sua cópia e distribuição com objectivos educacionais ou de investigação, não comerciais, desde que seja dado crédito ao autor e editor.

## Aknowledgments

I would like to express my gratitude to my supervisors M. Fátima Araújo (Centro de Ciências e Tecnologias Nucleares, C<sup>2</sup>TN) and Rui J.C. Silva (Faculdade de Ciências e Tecnologia da Universidade Nova de Lisboa, FCT-UNL) for all the support and especially to Elin Figueiredo, for all the guidance, attention, patience and sympathy during the most important stage of my academic life until now, always motivating me with interesting discussions and explanations about this whole new world and passion – the archaeometallurgy.

I also want to thank to the archaeologists Ana M. Bettencourt (Universidade do Minho, UM) and to João Fonte (Instituto de Ciencias del Patrimonio, Incipit/CSIC) for the support in the archaeological contextualization of the artefacts as well as to the archaeologist Beatriz Comendador Rey (Universidade de Vigo) for archaeometallurgical discussions. Also to the Director Isabel M. Cunha e Silva and the conservator Victor Hugo Torres of Museu Regional de Arqueologia D. Diogo de Sousa, in Braga, for allowing the study of the artefacts that made this investigation possible. To João Pedro Oliveira and Francisco Braz Fernandes (Centro de Investigação de Materiais/ Instituto de Nanoestruturas, Nanomodelação e Nanofabricação, CENIMAT/I3N) for the experimental X-ray diffraction by synchrotron radiation analyses in HEMS Beam Line at Petra III (Hamburg, Germany) and to CENIMAT/I3N for all the support given for the development of the work and its divulgation in the 5<sup>th</sup> Conference of the Quaternary, in 13<sup>th</sup> and 14<sup>th</sup> December 2013 at University of Porto.

I thank to the colleagues of C<sup>2</sup>TN for always receiving me with kindness and help me whenever I needed; to my school colleagues for the sharing of knowledge and experience during this 5 year journey, especially to those who became friends; and most of all to Departamento de Conservação e Restauro (DCR-FCT-UNL), mostly to all my teachers, for all the learning, not only scientifically but for making me grow as a person, as well as for the capacity of making my dreams become bigger and bigger.

I'm also grateful to my friends for all the joy and cherish, always supporting and believing in my capacities; to Rita for the unconditional presence and friendship and to Miguel for being the light on the darkest days, always helping me in all the possible ways; to my family, who always proudly supported my choices and celebrate my victories; to my father, for the daily care even far away the most of the time; to my brother for always standing by my side and making me feel the most loved person on earth; and to my mother, for always making me see that there is always more in me that I actually see or know and mostly... For everything!

As Nelson Mandela once said "It always seems impossible until it's done". Well, it's done!

And this is to all the impossible things!



## **Abstract**

This work presents the archaeometallurgical study of a group of metallic artefacts found in Moinhos de Golas site, Vila Real (North of Portugal), that can generically be attributed to Proto-history (1<sup>st</sup> millennium BC, Late Bronze Age and Iron Age).

The collection is composed by 35 objects: weapons, ornaments and tools, and others of difficult classification, as rings, bars and one small thin bent sheet. Some of the objects can typologically be attributed to Late Bronze Age, others are of more difficult specific attribution.

The archaeometallurgical study involved x-ray digital radiography, elemental analysis by micro-energy dispersive X-ray fluorescence spectrometry and scanning electron microscopy with energy dispersive spectroscopy, microstructural observations by optical microscopy and scanning electron microscopy. The radiographic images revealed structural heterogeneities frequently related with the degradation of some artefacts and the elemental analysis showed that the majority of the artefacts was produced in a binary bronze alloy (Cu-Sn) (73%), being others produced in copper (15%) and three artefacts in brass (Cu-Zn(-Sn-Pb)). Among each type of alloy there's certain variability in the composition and in the type of inclusions. The microstructural observations revealed that the majority of the artefacts suffered cycles of thermo-mechanical processing after casting.

The diversity of metals/alloys identified was a discovery of great interest, specifically due to the presence of brasses. Their presence can be interpreted as importations related to the circulation of exogenous products during the Proto-history and/or to the deposition of materials during different moments at the site, from the transition of Late Bronze Age/Early Iron Age (Orientalizing period) onwards, as during the Roman period.

## **Keywords**

Archaeometallurgy, Proto-history, Copper-based metals, Elemental composition, Manufacturing techniques



## **Resumo**

O presente trabalho apresenta o estudo arqueometalúrgico de um conjunto de artefactos metálicos encontrados no sítio de Moinhos de Golas, concelho de Vila Real (Norte de Portugal), podendo ser genericamente atribuído à Proto-história (1º milénio a.C., Idade do Bronze Final e Idade do Ferro).

A coleção é composta por 35 objetos: armas, artefactos de adorno e utensílios, entre outros de difícil atribuição – barras, argolas e uma pequena placa dobrada. Baseado nas tipologias, alguns artefactos podem ser atribuídos ao Bronze Final, sendo outros de difícil atribuição cronológica.

Foram efetuadas radiografias por raios X, análises elementares por micro-fluorescência de raios X por energias dispersivas, bem como observações microestruturais por microscopia ótica e eletrónica de varrimento. As imagens radiográficas revelaram heterogeneidades estruturais relacionadas frequentemente com a degradação de algumas peças e as análises elementares demonstraram que a maioria dos artefactos foi produzida numa liga de bronze binária (Cu-Sn) (73%), sendo de destacar o uso de outros metais/ligas, como alguns artefactos de cobre (15%) e três de latão (Cu-Zn(-Sn-Pb)). Cada tipo de liga apresenta uma certa variabilidade composicional e no tipo de inclusões existentes. As observações microestruturais revelam que a maioria dos artefactos sofreu ciclos de trabalho termomecânico após o vazamento em molde.

A diversidade de metais/ligas identificada foi uma descoberta de elevado interesse, especificamente devido à presença de latões. A presença de latões pode ser interpretada como resultado de uma circulação de materiais/objetos exógenos a partir da transição da Idade do Bronze Final para a Idade do Ferro (período Orientalizante), ou como uma deposição mais tardia, do período Romano.

## **Palavras-chave**

Arqueometalurgia, Proto-história, Ligas de cobre, Composição elementar, Técnicas de manufatura



## Index of contents

|   |      |
|---|------|
| Aknowledgments .....  | III  |
| Abstract .....  | V    |
| Resumo .....  | VII  |
| Index of Contents .....   | IX   |
| Index of Figures .....  | XI   |
| Index of Tables .....   | XIII |
| Symbols and Abbreviations .....   | XV   |
| 1. Introduction .....   | 1    |
| 2. Experimental .....   | 5    |
| 2.1. Digital X-Ray Radiography .....  | 6    |
| 2.2. Micro-Energy Dispersive X-Ray Fluorescence Spectrometry .....          | 6    |
| 2.3. Optical Microscopy .....   | 7    |
| 2.4. Scanning Electron Microscopy with Energy Dispersive Spectroscopy ..... | 7    |
| 3. Results and discussion .....   | 9    |
| 3.1 Macro and internal structural characterization of the artefacts .....   | 9    |
| 3.2. Elemental characterization .....                                       | 11   |
| 3.2.1. Metal composition of the artefacts .....                             | 11   |
| 3.2.2. Inclusions in the metallic matrix .....                              | 14   |
| 3.2.3. Influence of corrosion .....   | 16   |
| 3.3. Microstructural characterization .....                                 | 17   |
| 3.3.1. Manufacturing techniques .....                                       | 17   |
| 3.3.1.1. Weapons.....   | 18   |
| 3.3.1.2. Ornaments .....  | 19   |
| 3.1.1.3. Tools .....  | 19   |
| 3.1.1.4. Others – bars and rings .....                                      | 20   |
| 3.3.2. Intergranular corrosion .....  | 21   |
| 3.4. Some specificities of the collection .....                             | 21   |
| 3.4.1. Early brasses: the presence of two brass rings and a capsule .....   | 21   |
| 3.4.2. Joining metals in Antiquity: the case-study of the capsule .....     | 23   |
| 4. Conclusions .....  | 25   |
| References .....  | 27   |
| Appendices .....  | 31   |
| Appendix I. Artefacts details and particularities .....                     | 32   |
| Appendix II. Phase diagrams .....   | 34   |
| Appendix III. Microstructural characterisation of MG artefacts .....        | 36   |
| Appendix IV. Microstructures of the artefacts .....                         | 37   |
| Appendix IV. SEM-EDS analyses .....   | 38   |



## Index of Figures

|  |    |
|--|----|
| <b>Figure 1.</b> Moinhos de Golas site seen from East (A); Location of Moinhos de Golas in the Northwest Peninsula (B) (images adapted from Fonte <i>et al.</i> 2013). .....   | 2  |
| <b>Figure 2.</b> Metallic artefacts of the Moinhos de Golas site excluding rings. ....   | 3  |
| <b>Figure 3.</b> Rings grouped by diameter. ....   | 4  |
| <b>Figure 4.</b> Experimental design employed in the study of the artefacts. ....  | 5  |
| <b>Figure 5.</b> X-ray digital radiography of the pendants 2013-0449 (A) and 2013-0448 (B), the nail 2013-0447 (C), the bar 2013-0455 (D), the dagger 2013-0423 (E) and the tranchet 2013-0426 (F), next to a photograph of the tranchet taken before any conservation treatment (G). .... | 10 |
| <b>Figure 6.</b> X-Ray digital radiography of the dagger 2013-0425 (A) and its respective image by stereomicroscope (B), and X-ray radiography of the capsule (C) and (D). ....  | 10 |
| <b>Figure 7.</b> Relative frequencies of metal type in the analyzed copper-based artefacts. ....   | 12 |
| <b>Figure 8.</b> Histogram of Sn content in the studied copper-based artefacts. ....   | 12 |
| <b>Figure 9.</b> Micro-EDXRF spectra of the bent wire (represented in red) and the ring 02 (represented in green) of the artefact 2013-0428. ....  | 14 |
| <b>Figure 10.</b> SEM (BE) image and spot EDS analysis of the (1) Bi inclusion, (2) Ni-S inclusion and (3) Sn-O inclusion on the copper ring 2013-0434. ....   | 15 |
| <b>Figure 11.</b> SEM (BE) image and spot EDS analysis of the (1) metal matrix, (2) Zn-S inclusion and (3) globules of Pb on the brass ring 2013-0442. ....  | 15 |
| <b>Figure 12.</b> Microstructure of the ring 2013-0439 (A), the bar 2013-0453 (B) and the rivet 2013-0450 (C) (OM) showing ( $\alpha+\delta$ ) eutectoid, Cu-S inclusions among the $\alpha$ copper phase and dark colored inclusion inside the Cu-S inclusion. ....                       | 17 |
| <b>Figure 13.</b> Type of thermo-mechanical processing in the studied copper based artefacts. ....   | 18 |
| <b>Figure 14.</b> Microstructure of the daggers 2013-0423, 2013-0424 and 2013-0425 (OM). ....  | 18 |
| <b>Figure 15.</b> Microstructure of the nail 2013-0447, the pendant 2013-0448 and the pendant 2013-0449 (OM). ....   | 19 |
| <b>Figure 16.</b> Microstructure of the tranchet 2013-0426 (OM). ....  | 20 |
| <b>Figure 17.</b> Type of thermo-mechanical processing in the typology of the rings. ....  | 20 |
| <b>Figure 18.</b> Microstructure of the bar 2013-0451 with intergranular corrosion and the ring 2013-0443 with metallic copper. ....   | 21 |
| <b>Figure 19.</b> Table with Zn, Sn and Pb contents of brass objects from Moinhos de Gola and other early brasses from Spain, Eastern Mediterranean and Britain (Montero-Ruiz & Perea 2007 and Bayley 1990) and a ternary diagram considering these elements normalized to 100%. ....      | 23 |
| <b>Figure 20.</b> Superficial spot material over the corrosion products on the exterior of the capsule 2013-0457 by stereomicroscope (10x). ....   | 24 |
| <b>Figure 21.</b> SEM (BE) image and spot EDS analysis of the (1) remain of $\alpha$ primary grain, (2) $\alpha + \delta$ eutectoid and (3) corroded $\alpha$ -phase on the superficial spot material on base metal of the capsule 2013-0457. ....   | 25 |
| <b>Figure A1.</b> Decoration of the button 2013-0446 (A 7.5x; B 10x) under stereomicroscope. ....  | 32 |

|  |    |
|--|----|
| <b>Figure A2.</b> Detail of the marks present in the nail 2013-0447 under stereomicroscope (right 10x).....  | 32 |
| <b>Figure A3.</b> Detail of the horizontal rib of the tranchet 2013-0426 under stereomicroscope (right 10x).....   | 33 |
| <b>Figure A4.</b> Copper-tin phase diagram (Bulletin of Alloy Phase Diagrams Vol. 11 No. 3 1990).....  | 34 |
| <b>Figure A5.</b> Equilibrium and metastable phase diagrams for Cu-Sn system based on Centre Technique des Industries des Alliages Cuivreux. 1967. <i>Atlas Metallographique des Alliages Cuivreux</i> . Paris: Éditions Techniques des Industries de la Fonderie..... | 34 |
| <b>Figure A6.</b> Copper zinc phase diagram (Landolt-Börnstein. 1994. Phase Equilibria, Crystallographic and Thermodynamic Data of Binary Alloys, Volume 5: 1-11).....   | 35 |
| <b>Figure A7.</b> Microstructures of some of the MG collection artefacts.....  | 37 |
| <b>Figure A8.</b> SEM (BE) image and spot EDS analysis of the (1) $\alpha + \delta$ eutectoid, (2) Cu-S inclusion and (3) Cu-S-Fe inclusion on the bronze ring 2013-0431.....  | 38 |
| <b>Figure A9.</b> SEM (BE) image and spot EDS analysis of the (1) Metal matrix, (2) Cu-S inclusion and Ni and (3) Sn-O inclusion on the copper ring 2013-0435.....   | 38 |
| <b>Figure A10.</b> SEM (BE) image and spot EDS analysis of the (1) Metal matrix, (2) Zn-S inclusion and (3) Pb inclusion on the brass ring 2013-0441.....  | 38 |
| <b>Figure A11.</b> SEM (BE) image and spot EDS analysis of the (1) Pb inclusion with some Bi, (2) Bi inclusion and (3) Zn-S inclusion on the capsule 2013-0457.....  | 39 |

## Index of Tables

|   |    |
|---|----|
| <b>Table 1.</b> Quantification limits for micro-EDXRF analyses of copper-based alloys adopted from Figueiredo <i>et al.</i> 2013a and Valério <i>et al.</i> 2014.....   | 6  |
| <b>Table 2.</b> Accuracy of the micro-EDXRF quantitative analyses (average $\pm$ one standard deviation for 3 spot analyses) (accuracy calculated as ((Obtained value-certified value)/certified value) x 100).....   | 7  |
| <b>Table 3.</b> Experimental results on the copper-based artefacts (the composition is given by average of three micro-EDXRF analyses $\pm$ standard deviation).....  | 11 |
| <b>Table 4</b> Summary of the experimental results relative to the SEM-EDS analysis on the metal inclusions.....  | 15 |
| <b>Table 5.</b> Summary of the experimental results relative to the corrosion influence on the different type of alloys.....  | 16 |
| <b>Table 6.</b> Results of elemental analysis performed over corrosion on the artefact found in Casa da Orca (Castro Nunes <i>et al.</i> 1989) and the capsule found in the present collection. ....  | 23 |
| <b>Table 7.</b> Results of micro-EDXRF analyses made over the superficial spot material on base metal and corrosion of the capsule 2013-0457.....   | 24 |
| <b>Table A1.</b> OM characterization of the copper-based artefacts (*: % given by micro-EDXRF; †: Influence of corrosion; C: Casting; D: Deformation/forging; T: heat treatment/annealed; ↓ low amount; ↑ high amount; other: other small dark inclusion, possibly Cu-S-Fe in bronzes and Sn-O in coppers)..... | 36 |



## **Symbols and Abbreviations**

**AD** Anno Domini

**BA** Bronze Age

**BC** Before Christ

**BCS** British Chemical Standards

**BF** Bright field (in OM observations)

**CA** Chalcolithic

**CENIMAT** Centro de Investigação em Materiais

**C<sup>2</sup>TN/IST** Centro de Ciências e Tecnologias Nucleares, Instituto Superior Técnico

**DCR** Departamento de Conservação e Restauro

**EIA** Early Iron Age

**EDXRF** Energy Dispersive X-Ray Fluorescence

**FCT** Faculdade de Ciências e Tecnologia

**I3N** Instituto de Nanoestruturas, Nanomodelação e Nanofabricação

**IA** Iron Age

**IP** Iberian Peninsula

**LBA** Late Bronze Age

**MBA** Middle Bronze Age

**MG** Moinhos de Golas

**NBS** National Bureau of Standards

**OM** Optical Microscopy

**POL** Polarized light (in respect to OM observations)

**SE** Secondary electrons

**SEM-EDS** Scanning Electron Microscopy – Energy Dispersive Spectroscopy

**UNL** Universidade Nova de Lisboa

## 1. Introduction

When compared to the use of pure metals, the intentional fabrication and use of alloys can be understood as a major innovation process, as it relates with the improvement of the material properties, such as changing its hardness, providing different colors, higher castability when compared with the individual metals of the alloy. In the group of copper-based materials, bronze can probably be the most common alloy in the Proto-history (Craddock 1995), showing more strength and hardening capacities by cold work deformation than the pure copper (Tylecote 1992).

Bronze was progressively introduced in the Portuguese territory during the Bronze Age (BA), which is traditionally divided in 3 periods: the Early Bronze Age (EBA ~2300-1500 cal BC), the Middle Bronze Age (MBA ~1500-1250 cal BC) and the Late Bronze Age (LBA ~1250-850 cal BC) (Ruiz-Galvez 2014). In some regions, namely in the center/northern Portugal the LBA is frequently assigned until a later chronology, as until the VI century BC (Senna-Martinez 2010). It was only in the MBA that the bronzes began to appear with some regularity in the Portuguese territory, becoming frequent during LBA, when binary bronzes were the main alloy used (Vilaça 1997; Vilaça 2006). During this period a diversification in typologies happened and artefacts with more complex shapes began to be produced. This could be a result of technological improvements in the cast operation namely, the use of multifaceted moulds and the pre heating of the moulds before pouring (Rovira 2004).

During this last period in the Portuguese territory there were also relationships with other regions belonging to Atlantic and Mediterranean traditions (Ruiz-Galvez 1998). The increase of the contacts culminated with the settlement of Phoenician colonies at least during the VIII century BC (Arruda 2008). This gave rise to the so called Orientalizing period, a period characterized by the introduction of new cultural and technological traditions brought by Mediterranean people, that later reached more interior and northern Portuguese regions, where the LBA traditions seem to last longer (Arruda 2008).

Archaeometallurgy is an archaeometric field that relies on the scientific study of archaeological metals by studying metallic evidences - like artefacts - as well as residual products – like slags, crucibles and moulds (Centre for Archaeology Guidelines 2001). These scientific studies are crucial for understanding the importance and evolution of the metallurgical activities, as well as the culture, economy and the technological capacities and exchanges of the people and communities (Craddock 1995).

The archaeometallurgical field had great developments during the second half of the XX century with the development of large scale projects as the “Studien zu den Anfängen der Metallurgie” (SAM) where thousands of samples of prehistoric copper-based artefacts from all Europe, including the Iberian Peninsula (IP), were collected and analyzed (Junghans *et al.* 1968; 1974). In the Portuguese territory, studies concerning chemical composition of Pre and Proto-historic metallic artefacts improved considerably due to the installation of non-destructive techniques in various research centers since the seventies of the late century (Araújo *et al.* 2013). Many of these studies comprise copper-based, gold and silver artefacts from significant chronological contexts from the Chalcolithic (CA) to Early Iron Age (EIA) (Araújo *et al.* 2004; Canha *et al.*,

2007; Figueiredo *et al.* 2007, 2010, 2012; Melo *et al.* 2009; Silva *et al.* 2008; Soares *et al.* 2004, 2010; Vilaça 1997; Valério *et al.* 2006, 2007a,b).

In the present work it is presented the archaeometallurgical study of the metallic collection of Moinhos de Golas (MG) (Solveira, Montalegre, Vila Real), which context and finding conditions were published recently (Fonte *et al.* 2013).

The archaeological site was discovered in 2013, is positioned at a relatively high hill (maximum altitude of 843 meters) at the left side of de Assureira river, and has large size stones that naturally emphasize the site (Fig. 1). Ceramics and metallic artefacts were found on the site, which were integrated in the Museu Regional de Arqueologia D. Diogo de Sousa, in Braga, where they were submitted to conservation treatments.



**Figure 1.** Moinhos de Golas site seen from East (A); Location of Moinhos de Golas in the Northwest Peninsula (B) (images adapted from Fonte *et al.* 2013).

The metallic collection is composed by 35 objects (Fig. 2 and 3) including 3 weapons (daggers of different sizes and shapes), 5 ornaments (one button, two possible pendants, one nail and a small capsule), 1 tool (one tranchet), as well as others of difficult classification such as 17 rings and 8 bars (of different sizes and shapes, that include one object composed by one wire and two rings) and one small thin folded sheet.<sup>1</sup>

The daggers have different sizes and shapes that could be related to different utilitarian purposes or aesthetical motivations. This kind of objects is relatively frequent among LBA deposits (Vilaça 2006).

The button (2013-0446) has the particularity of having small printed marks on its outer surface that appears to be a decoration, possibly made after casting with some kind of pointed tool (see Fig. A1 – Appendix I). In some regions this decoration is faded by the corrosion products. The nail (2013-0447) does also have two marks on the head (see Fig. A2 – Appendix I), of unknown origin or purpose.

The tranchet (2013-0426) is a particular object not only within the collection, but also among LBA contexts of the Western IP, since only about twenty objects of this kind are known (Vilaça

<sup>1</sup>The typological classification presented in this work shows some differences from the initially proposed in Fonte *et al.* 2013 as a result of the detailed archaeometallurgical study that allowed a better examination and study of the artefacts.

2009). This tranche has one side completely flat and the other has a horizontal rib, where the blade begins (see Fig. A3 – Appendix I). This type is mostly common in the center of the Portuguese territory (Vilaça 2009). The functional purpose of this kind of object is still under discussion. It's not known if it was used for cutting flexible solids as leather, used as shaving razors or even as possible mirrors (Vilaça 2009).

The two bars 2013-0450 and 2013-0451 show flat surfaces on their tops, suggesting their use as rivets. Rivets were a common way of assembling different parts of an object during de LBA (Figueiredo *et al.* 2011a). The rest of the bars, of various sizes and circular or near-quadrangular cross-sections (2013-0427, 2013-0452 to 2013-0455) could be parts of other objects, semi-finished products, as the bars 0453 and 0454 that could be awls. The small sheet 2013-0456 is very thin and that's probably why it's bent. The specific purpose of this object is also unknown.

The 17 rings can be grouped according to their diameter sizes, ~3 cm, ~2 cm and <2 cm, being composed by 4, 7 and 6 rings respectively (Fig. 3). The group of the largest diameter rings is the one that presents the thinnest metal cross-section. Rings have been found in various Proto-historic contexts, and in the Portuguese territory one can mention the relatively large collection of 32 rings from Medronhal attributed to around the VIII century BC (Figueiredo *et al.* 2013a) comprising the transition of LBA to Iron Age (IA). Their specific purpose is yet a question with no answer. They could be cloth or hair accessories (the dimensions of some of them and thickness of the smallest rings in the collection exclude the purpose of finger rings), or even a part of another object, as the example of the artefact 2013-0428, that is composed by a wire with a ring fastened in each end.



**Figure 2.** Metallic artefacts of the Moinhos de Golas site excluding rings.



**Figure 3.** Rings grouped by diameter.

A preliminary study on 13 artefacts of the collection by hand-held X-ray fluorescence has been performed previously to provide a first insight into the type of alloys present in the collection (Fonte *et al.* 2013). This study revealed the presence of binary bronzes, raised a question about the possible presence of ternary bronzes and showed the presence of one copper object (the bent sheet). Despite providing some bases for the archaeological/cultural context of the collection, the study had great limitations since the analysis were performed over the corroded surfaces of the artefacts and small or thin artefacts could not be analyzed, excluding, for example, the rings that compose almost half of the artefacts collection.

In the present archaeometallurgical study, a combination of analytical and examination techniques that provides complementary information about the artefacts, namely compositional, macro and micro structural characterizations will be presented and discussed. The discussion will involve the identification of the materials and manufacturing processes in order to contribute to a better understanding of the history and the technology of the past societies as well as the use of primitive materials and their degradation.

## 2. Experimental

All the artefacts were first analyzed by digital X-ray radiography to investigate the internal structure. The majority was analyzed by micro-energy dispersive X-ray fluorescence spectrometry (micro-EDXRF), scanning electron microscopy with energy dispersive spectroscopy (SEM-EDS) and examined by optical microscopy (OM) to define the type of alloy and the manufacturing processes involved on the production of the objects, as well as to evaluate some degradation processes that can have implications on the future preservation of the collection.

Since the archaeological copper-based artefacts remained buried for a long period of time they have a superficial corrosion layer with different composition when compared to the original metal. Corrosion processes originated by different electrochemical potentials and diverse stabilities of the corrosion products formed (Robbiola & Portier 2006) will significantly affect the metal analysis by micro-EDXRF. Besides this, the surface can be contaminated by soil elements (the effects of corrosion on the metal alloys studied will be described on section 3.2.3.). For this specific reason, it's necessary to remove the alteration layers at the surface to make possible the analysis of the unaltered metal. Thus, the elemental composition determined by micro-EDXRF on the artefacts was obtained at a small surface previously cleaned. These cleaned areas were also analyzed by SEM-EDS and observed under OM. Only two artefacts were not cleaned due to their fragile conservation state being the results of the analyses only considered semi-quantitatively.

Additionally, the majority of the copper-based artefacts in this study were characterized by OM observations on the same small cleaned areas to identify different phases, inclusions and other microstructural features related to specific manufacturing sequences. The characterization of the inclusions was assisted by SEM-EDS analyses on a few selected artefacts. In Figure 4, a scheme of the experimental design is shown.

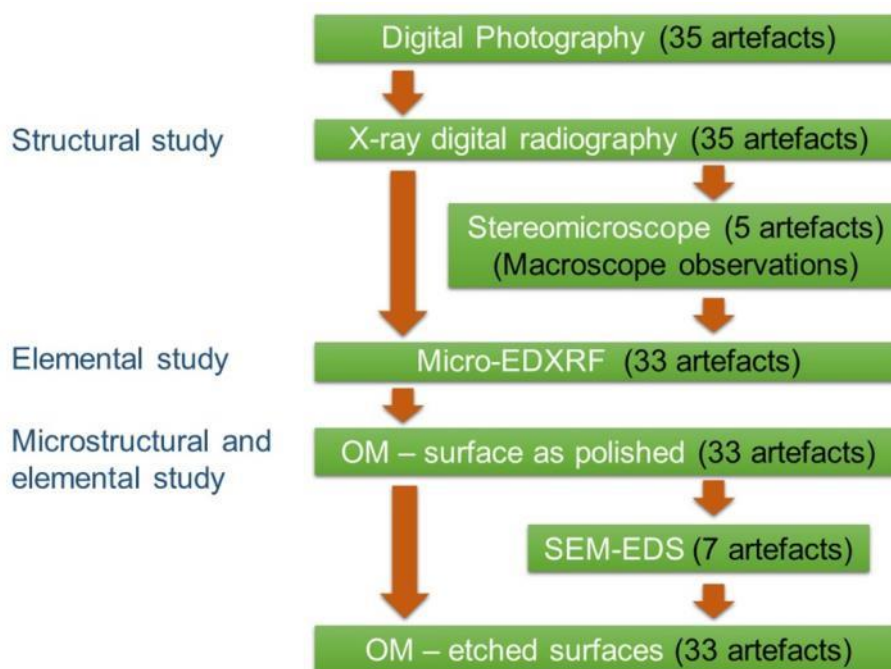


**Figure 4.** Experimental design employed in the study of the artefacts.

## 2.1. Digital X-Ray Radiography

Digital X-ray radiography was applied in all artefacts to investigate internal heterogeneities that could be related to specific manufacturing techniques, like the joining of metallic elements, or to the alteration/corrosion of metal.

The radiographic images were obtained with a digital X-ray system, ArtXRay, SEZ Series, manufactured by NTB GmbH (Dickel, Germany), installed at the DCR-FCT-UNL. The parameters used were a voltage of 130 kV and current intensity of 3.7 mA (480 W), that consists of the maximum power capacity of the equipment. This was adequate for the internal and macro structural study of most artefacts, especially for those of thinner cross-sections.

The set-up of the analysis involved a focus-detector distance of 1.36 m, with the artefacts positioned within a distance of circa 14 cm from the detector. The image processing involved the iX/Pect software.

The use of this equipment for the study of archaeological metals has been previously published (Figueiredo *et al.* 2011a), showing its relevance in the study of ancient manufacturing techniques involving the joining of different pieces of metal. In the present work it was also used for the study of internal heterogeneities which may be connected to degradation/corrosion phenomena (Guidelines on the X-radiography of archaeological metalwork 2006).

## 2.2. Micro-Energy Dispersive X-Ray Fluorescence Spectrometry

Micro-EDXRF analyses were performed in most metal artefacts to determine the metal alloy composition in a small area free from the superficial corrosion layers. These areas were metallographically prepared with a minicraft equipped with a rotary point of cotton impregnated with diamond paste (6  $\mu\text{m}$  until  $\frac{1}{4}$   $\mu\text{m}$ ), allowing the removal of the superficial corrosion layers in a small area (<5 mm<sup>2</sup>).

The micro-EDXRF analysis were performed in an ArtTAX Pro spectrometer installed at DCR-FCT-UNL, which comprises: a low-power X-ray tube with a Mo anode; a set of polycapillary lens that generate a micro spot of ~70  $\mu\text{m}$  in diameter of primary radiation; an integrated CCD camera and three beam-crossing diodes that provide the control over the exact position on the sample to be analyzed; and a silicon drift electro-thermally cooled detector with a resolution of 160 eV at Mn-K $\alpha$  (Bronk *et al.* 2001). The artefacts were analyzed in 3 different spots in the prepared areas using 40 kV, 0.5 mA and 100 s of tube voltage, current intensity and live time respectively.

The analytical procedure followed an established procedure for archaeological metals using this specific equipment, and published previously in detail (Figueiredo *et al.* 2013a; Valério *et al.* 2014) and quantification limits were adopted from there (Table 1).

**Table 1.** Quantification limits for micro-EDXRF analyses of copper-based alloys adopted from Figueiredo *et al.* 2013a and Valério *et al.* 2014.

| Cu    | Sn   | Pb    | As    | Fe    | Ni    |
|-------|------|-------|-------|-------|-------|
| 0.04% | 0.5% | 0.10% | 0.10% | 0.05% | 0.07% |

Quantitative analysis were made using Winaxil software that uses fundamental parameter method and experimental calibration factors that were calculated with certified reference

materials: Phosphor Bronze 551 Spectrographic Standard from British Chemical Standards (BCS) for the copper and tin (bronze) alloys, and Free-Cutting Brass 1103 from National Bureau of Standards (NBS), for the copper and zinc (brass) alloys.

The determination of the accuracy of the analytical procedure was accomplished by the analysis and quantification of another certified reference material (Phosphor Bronze 552 from BCS, for the bronze alloys, and Free-Cutting Brass 1104 from NBS for the brass alloys) using the same experimental conditions (Table 2). As it's observed in Table 2, the experimental errors are relatively low for the major elements, as for Cu and Sn in the bronze alloys, and Cu and Zn for the brasses, and higher for the minor elements (as Pb, Ni and Fe).

**Table 2.** Accuracy of the micro-EDXRF quantitative analyses (average  $\pm$  one standard deviation for 3 spot analyses) (accuracy calculated as  $((\text{Obtained value}-\text{certified value})/\text{certified value}) \times 100$ ).

| BCS SS552         | Cu             | Sn              | Pb              | Fe              | Ni              | Zn              |
|-------------------|----------------|-----------------|-----------------|-----------------|-----------------|-----------------|
| Certified (wt. %) | 87.7           | 9.78            | 0.63            | 0.10            | 0.56            | 0.35            |
| Obtained (wt. %)  | 88.6 $\pm$ 0.2 | 9.70 $\pm$ 0.10 | 0.61 $\pm$ 0.09 | 0.11 $\pm$ 0.02 | 0.56 $\pm$ 0.03 | 0.45 $\pm$ 0.01 |
| Relative error    | 1%             | -0.8%           | -3%             | 13%             | 0.6%            | 30%             |
| NBS 1112          | Cu             | Sn              | Pb              | Fe              | Ni              | Zn              |
| Certified (wt. %) | 61.33          | 0.43            | 2.77            | 0.088           | 0.07            | 35.31           |
| Obtained (wt. %)  | 61.6 $\pm$ 0.2 | 0.45 $\pm$ 0.01 | 2.67 $\pm$ 0.07 | 0.09 $\pm$ 0.00 | 0.08 $\pm$ 0.01 | 35.1 $\pm$ 0.2  |
| Relative error    | -0.5%          | 4%              | -3%             | -0.1%           | 11%             | -0.6%           |

### 2.3. Optical Microscopy

The OM observations were conducted in a Leica DMI5000M microscope installed at CENIMAT/I3N-FCT-UNL. This microscope is coupled to a computer with the LAS V2.6 software which allows the use of multifocus functionality, essential to the observation of less flat surfaces as the ones resulting of metallographic manual and located preparation (Figueiredo *et al.* 2013b). This feature added to the characteristic of inverted lenses allows the examination of small prepared areas of large size artefacts without the need of sampling.

Initially, the microstructure examinations were made in bright field (BF) and under polarized light (Pol) with the surface in as-polished state. The Pol observations allowed the study of some corrosion features due to specific colors that corrosion products can show under this type of illumination. After these observations, the surfaces were etched with an aqueous ferric chloride solution (prepared according to Scott 1991: 120 ml of distilled water, H<sub>2</sub>O; 30 ml of hydrochloric acid, HCL; and 10 g of ferric chloride, FeCl<sub>3</sub>) in order to reveal microstructural features like grain boundaries, annealing twins and slip bands among the grains, that are important features to characterize specific thermo-mechanical treatments that have been performed to shape the artefacts.

### 2.4. Scanning Electron Microscopy with Energy Dispersive Spectroscopy

SEM-EDS analyses were performed on some selected items, on the small area free of corrosion products, for the identification of metallic phases and for the study of the inclusions present in the metallic matrix.

The SEM analyses were performed in a Zeiss equipment, model DSM 962, installed at CENIMAT/I3N/FCT/UNL, which has backscattered electrons (BSE) and secondary electrons

(SE) imaging modes and an energy dispersive spectrometer (EDS) from Oxford Instruments model INCAx-sight with an ultra-thin window, able to detect low atomic number elements as oxygen and carbon. Elemental semi-quantifications were made using a ZAF procedure.

The analyses were performed before etching the surface for the OM observations and without any superficial conductive coating (such as a carbon or gold) following an experimental procedure previously developed for archaeological metals and published in Figueiredo *et al.* 2011b.

### 3. Results and discussion

#### 3.1. Macro and internal structural characterization of the artefacts

The radiographic images were worked digitally so that the darkest areas correspond to higher thicknesses and/or materials with a higher attenuation coefficient (which depends on the energy of the radiation, the elements present and the density of the material, in such a way that generally higher atomic number elements and/or denser materials would show higher attenuations)<sup>2</sup>. The images allowed the observations of fragile areas, as fissures and/or cracks in some of the artefacts, however in the thickest objects no radiation was transmitted, resulting in opaque images, not workable.

The X-ray digital images of the possible pendants 2013-0448 (Fig. 5 B) and 2013-0449 (Fig. 5 A) show two opaque images, possibly related to these being compact objects as could also be proposed by their relatively high mass. There's also no clear evidence of the joining of the pin and the head in these artefacts. However, the pin and the head have a similar composition, as proven by the micro-EDXRF analyses (see section 3.2.1.), which can suggest that they were actually cast as one object.

The radiographic images of the nail 2013-0447 taken in different positions (Fig. 5 C) do not evidence any joining of the head and pin, what could suggest that this artefact resulted from a single cast. Macroscopic observations of the pin surface and shape show that it only acquires a near-quadrangular cross-section in the outer half length (outside the head), possibly the area where it was possible to work after the casting/shaping of the head.

On the bending area of the small bar 2013-0455 (Fig. 5 D) it's possible to see a fissure that can probably be related to internal tensions caused by the manufacture processes, namely by the deformation required to bend the bar.

Regarding the dagger 2013-0423 (Fig. 5 E), a denser zone on the center of the object is observed, which corresponds to a central rib of a greater thickness than the blade, which extends from near the hole made to the placement of the rivet on the hilt until the end of the dagger. There is also a fissure on the top of the handle that appears to be located in the area where originally the beginning of a hilt was positioned, suggesting that this area could have been subjected to some pressure/tensions leading to the development of fissures. Besides this, there were observed some heterogeneities along the blade, of semi-circular shape, that correspond to areas of stronger corrosion and some loss of material. On the tranchet 2013-0426 (Fig. 5 F) the radiographic image pointed out to two distinct areas on the blade: one darker zone, at left (pointed out with an arrow on the figure) and other more heterogeneous, at right and comprising the inferior zone of the edge, with similar patterns as those observed in the blades of the dagger. These differences are not related to major compositional heterogeneities of the artefact metal (see section 3.2.1. with various analysis on the artefact) neither to significant differences in thickness, but could possibly be related to different corrosion degrees that developed in the artefact, as it can be observed in the photograph taken of the artefact before any conservation treatment where the existence of a superficial corrosion layer, more thick, and possibly more protective, is present at the left superior zone of the artefact which probably prevented a deep corrosion of this area (visible at the Fig. 5 G).

---

<sup>2</sup> <http://physics.nist.gov/PhysRefData/XrayMabssCoef/chap2.html>

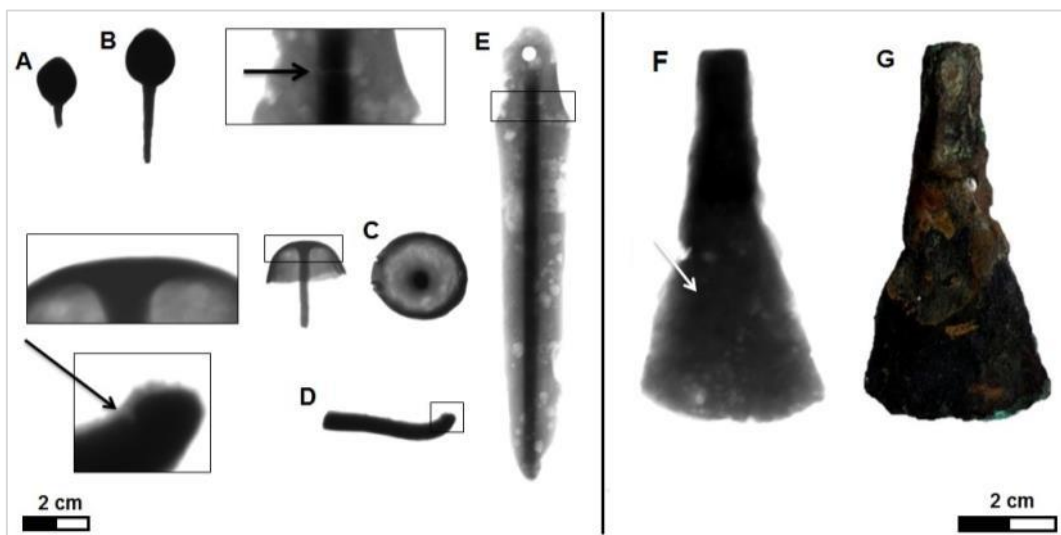


**Figure 5.** X-ray digital radiography of the pendants 2013-0449 (A) and 2013-0448 (B), the nail 2013-0447 (C), the bar 2013-0455 (D), the dagger 2013-0423 (E) and the tranchet 2013-0426 (F), next to a photograph of the tranchet taken before any conservation treatment (G).

The X-Ray image of the dagger 2013-0425 (Fig. 6 A) allows the observation of an external corrosion layer, as well as the presence of two fissures, one of them at the bottom area of the blade, and the other one, smaller, at the top, similar in its location to the one found in the dagger 2013-0423 (Fig. 5 E). Also, at the top of this dagger it's possible to see the presence of three circles. Analyses by micro-EDXRF were made at the corresponding areas of these circles at the superficial corrosion products and the spectra showed no differences from spectra obtained on the surface of the rest of the object. Investigation under a stereomicroscope with different incident lights wasn't either conclusive, however suggested a slightly lower thickness in these areas.

The radiographic image of the metallic capsule 2013-0457 clearly showed a fissure at one edge that had not been detected earlier and a small dark spot, depicted on the Figure 6 (C). This small spot showed correspondence to a material on the outer surface of the capsule, which was detected visually with some difficulty. This material was later subjected to a detailed study by SEM-EDS (see section 3.4.2.). In the radiographic image it was also possible to observe some material/soil depositions inside the object (Fig. 6 D).

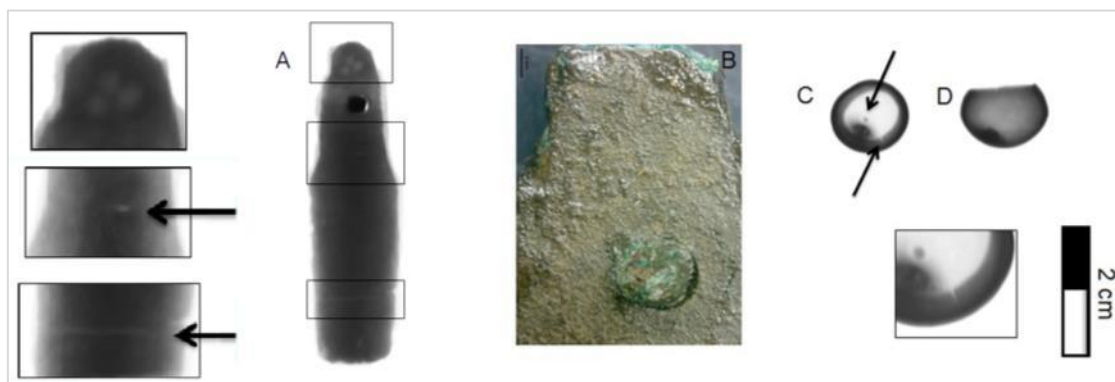


**Figure 6.** X-Ray digital radiography of the dagger 2013-0425 (A) and its respective image by stereomicroscope (B), and X-ray radiography of the capsule (C) and (D).

## 3.2. Elemental characterization

### 3.2.1. Metal composition of the artefacts

The results of the micro-EDXRF analysis (Table 3) show that most of the artefacts are made by a binary bronze alloy (Cu-Sn alloy) and six objects are made in copper (3 rings, 2 bent bars, one of them from the object 2013-0428, and one bent sheet) having three of them low amounts of Sn (~1% Sn). The remaining three objects (a capsule and two rings) are made in a copper alloy with zinc (contents 9-19% Zn), being thus generically called brasses. Among these 3 objects, the two rings do also show variable amounts of other elements, namely Sn (~3-4%) and Pb (one with ~7%), which can therefore designate them as gunmetal or leaded gunmetal (see details on this alloys on section 3.4.1) (Fig. 7).

**Table 3.** Experimental results on the copper-based artefacts (the composition is given by average of three micro-EDXRF analyses  $\pm$  standard deviation).

| Reference | Artefact |                 | micro-EDXRF (wt. %) |                |                 |                 |                |                        | Metal  |
|-----------|----------|-----------------|---------------------|----------------|-----------------|-----------------|----------------|------------------------|--------|
|           |          |                 | Cu                  | Sn             | Pb              | As              | Fe             | Zn                     |        |
| 2013-0423 | Dagger   | Blade           | 86.7 $\pm$ 1.1      | 12.8 $\pm$ 1.2 | 0.3 $\pm$ 0.1   | <0.10           | <0.05          | n.d.                   | Bronze |
|           |          | Center*         | 69.7 $\pm$ 2.0      | 29.9 $\pm$ 2.0 | 0.2 $\pm$ 0.0   | <0.10           | <0.05          | n.d.                   | Bronze |
|           |          | Top*            | 80.8 $\pm$ 4.4      | 18.8 $\pm$ 4.4 | 0.2 $\pm$ 0.0   | <0.10           | <0.05          | n.d.                   | Bronze |
| 2013-0424 | Dagger   | Blade           | 85.6 $\pm$ 0.7      | 13.7 $\pm$ 0.9 | 0.5 $\pm$ 0.1   | <0.10           | <0.05          | n.d.                   | Bronze |
|           |          | Center          | 87.2 $\pm$ 1.0      | 12.2 $\pm$ 1.0 | 0.4 $\pm$ 0.0   | <0.10           | <0.05          | n.d.                   | Bronze |
| 2013-0425 | Dagger   | Top             | 86.1 $\pm$ 0.4      | 13.3 $\pm$ 0.5 | 0.4 $\pm$ 0.0   | <0.10           | <0.05          | n.d.                   | Bronze |
|           |          | Tranchet Blade* | 84.4 $\pm$ 1.1      | 15.3 $\pm$ 1.1 | 0.2 $\pm$ 0.0   | <0.10           | <0.05          | n.d.                   | Bronze |
| 2013-0426 |          | p1              | 85.1 $\pm$ 0.3      | 14.9 $\pm$ 0.3 | n.d.            | <0.10           | <0.05          | n.d.                   | Bronze |
|           |          | p2              | 84.5 $\pm$ 0.4      | 15.5 $\pm$ 0.5 | n.d.            | <0.10           | <0.05          | n.d.                   | Bronze |
|           |          | Top             | 85.2 $\pm$ 0.3      | 14.7 $\pm$ 0.3 | n.d.            | <0.10           | <0.05          | n.d.                   | Bronze |
| 2013-0427 | Bar      | Wire            | 84.1 $\pm$ 3.3      | 13.8 $\pm$ 0.3 | n.d.            | 0.09 $\pm$ 0.01 | <0.05          | n.d.                   | Bronze |
|           |          | Wire            | 99.9 $\pm$ 2E-14    | n.d.           | n.d.            | <0.10           | <0.05          | n.d.                   | Copper |
| 2013-0428 | Ring     | Ring 01         | 86.5 $\pm$ 0.3      | 13.2 $\pm$ 0.3 | n.d.            | 0.19 $\pm$ 0.01 | <0.05          | n.d.                   | Bronze |
|           |          | Ring 02         | 86.3 $\pm$ 0.2      | 13.5 $\pm$ 0.1 | n.d.            | 0.12 $\pm$ 0.01 | <0.05          | n.d.                   | Bronze |
| 2013-0429 | Ring     | 87.4 $\pm$ 0.4  | 12.7 $\pm$ 0.2      | n.d.           | <0.10           | <0.05           | n.d.           | Bronze                 |        |
| 2013-0430 | Ring     | 88.2 $\pm$ 0.6  | 11.8 $\pm$ 0.6      | n.d.           | n.d.            | <0.05           | n.d.           | Bronze                 |        |
| 2013-0431 | Ring     | 86.8 $\pm$ 0.1  | 13.0 $\pm$ 0.1      | n.d.           | <0.10           | <0.05           | n.d.           | Bronze                 |        |
| 2013-0434 | Ring     | 98.4 $\pm$ 0.6  | 1.3 $\pm$ 0.6       | n.d.           | 0.10 $\pm$ 0.03 | 0.05 $\pm$ 0.08 | n.d.           | Copper                 |        |
| 2013-0435 | Ring     | 98.8 $\pm$ 0.3  | 1.2 $\pm$ 0.3       | n.d.           | n.d.            | <0.05           | n.d.           | Copper                 |        |
| 2013-0436 | Ring     | 87.8 $\pm$ 1.3  | 12.0 $\pm$ 1.2      | n.d.           | 0.11 $\pm$ 0.01 | <0.05           | n.d.           | Bronze                 |        |
| 2013-0437 | Ring     | 99.9 $\pm$ 0.0  | n.d.                | n.d.           | <0.10           | <0.05           | n.d.           | Copper                 |        |
| 2013-0438 | Ring     | 85.2 $\pm$ 0.9  | 14.6 $\pm$ 0.9      | n.d.           | 0.13 $\pm$ 0.01 | <0.05           | n.d.           | Bronze                 |        |
| 2013-0439 | Ring     | 85.8 $\pm$ 0.6  | 13.8 $\pm$ 0.5      | 0.2 $\pm$ 0.1  | <0.10           | <0.05           | n.d.           | Bronze                 |        |
| 2013-0440 | Ring     | 85.3 $\pm$ 0.6  | 14.5 $\pm$ 0.6      | 0.1 $\pm$ 0.0  | <0.10           | <0.05           | n.d.           | Bronze                 |        |
| 2013-0441 | Ring     | 82.0 $\pm$ 1.0  | 2.9 $\pm$ 0.1       | 0.3 $\pm$ 0.1  | <0.10           | 0.35 $\pm$ 0.01 | 14.5 $\pm$ 1.0 | Brass/Gunmetal         |        |
| 2013-0442 | Ring     | 79.7 $\pm$ 3.2  | 3.5 $\pm$ 0.5       | 7.2 $\pm$ 2.8  | <0.10           | 0.28 $\pm$ 0.02 | 9.1 $\pm$ 0.7  | Brass/ Leaded Gunmetal |        |
| 2013-0443 | Ring     | 89.0 $\pm$ 1.6  | 10.6 $\pm$ 1.5      | 0.3 $\pm$ 0.1  | <0.10           | <0.05           | n.d.           | Bronze                 |        |
| 2013-0444 | Ring     | 85.8 $\pm$ 1.0  | 13.6 $\pm$ 1.0      | 0.3 $\pm$ 0.0  | 0.12 $\pm$ 0.01 | <0.05           | n.d.           | Bronze                 |        |
| 2013-0445 | Ring     | 90.7 $\pm$ 0.9  | 8.1 $\pm$ 0.8       | 0.8 $\pm$ 0.1  | 0.21 $\pm$ 0.02 | <0.05           | n.d.           | Bronze                 |        |
| 2013-0446 | Button   | Side            | 85.7 $\pm$ 0.2      | 14.0 $\pm$ 0.2 | 0.1 $\pm$ 0.0   | 0.05 $\pm$ 0.01 | <0.05          | n.d.                   | Bronze |
|           |          | Interior        | 87.7 $\pm$ 0.6      | 12.0 $\pm$ 0.7 | 0.2 $\pm$ 0.0   | <0.10           | <0.05          | n.d.                   | Bronze |
| 2013-0447 | Nail     | Head            | 87.6 $\pm$ 1.1      | 12.0 $\pm$ 1.1 | 0.2 $\pm$ 0.1   | <0.10           | <0.05          | n.d.                   | Bronze |
|           |          | Pin             | 89.8 $\pm$ 0.5      | 10.0 $\pm$ 0.5 | 0.1 $\pm$ 0.1   | <0.10           | <0.05          | n.d.                   | Bronze |
| 2013-0448 | Pendant  | Head            | 86.4 $\pm$ 0.1      | 13.2 $\pm$ 0.1 | 0.2 $\pm$ 0.0   | <0.10           | <0.05          | n.d.                   | Bronze |
|           |          | Pin             | 86.4 $\pm$ 0.2      | 13.3 $\pm$ 0.2 | n.d.            | <0.10           | <0.05          | n.d.                   | Bronze |
| 2013-0449 | Pendant  | Head            | 88.4 $\pm$ 1.5      | 12.3 $\pm$ 1.5 | 0.1 $\pm$ 0.1   | <0.10           | <0.05          | n.d.                   | Bronze |
|           |          | Pin             | 87.2 $\pm$ 0.2      | 12.6 $\pm$ 0.2 | 0.1 $\pm$ 0.0   | <0.10           | <0.05          | n.d.                   | Bronze |
| 2013-0450 | Bar      | 86.9 $\pm$ 1.04 | 13.0 $\pm$ 1.1      | n.d.           | <0.10           | <0.05           | n.d.           | Bronze                 |        |
| 2013-0451 | Bar      | 87.8 $\pm$ 0.8  | 12.0 $\pm$ 0.8      | n.d.           | 0.14 $\pm$ 0.01 | <0.05           | n.d.           | Bronze                 |        |
| 2013-0452 | Bar      | 87.9 $\pm$ 0.7  | 11.9 $\pm$ 0.7      | n.d.           | 0.15 $\pm$ 0.01 | <0.05           | n.d.           | Bronze                 |        |
| 2013-0453 | Bar      | 98.4 $\pm$ 0.2  | 1.3 $\pm$ 0.3       | n.d.           | <0.10           | <0.05           | n.d.           | Copper                 |        |
| 2013-0454 | Bar      | 94.7 $\pm$ 0.9  | 4.9 $\pm$ 0.9       | 0.2 $\pm$ 0.1  | <0.10           | <0.05           | n.d.           | Bronze                 |        |
| 2013-0455 | Bar      | 87.6 $\pm$ 0.8  | 12.1 $\pm$ 0.8      | 0.2 $\pm$ 0.1  | <0.10           | <0.05           | n.d.           | Bronze                 |        |
| 2013-0456 | Sheet    | 99.1 $\pm$ 0.1  | n.d.                | 0.1 $\pm$ 0.0  | 0.75 $\pm$ 0.02 | <0.05           | n.d.           | Copper                 |        |
| 2013-0457 | Capsule  | 79.0 $\pm$ 1.0  | n.d.                | 0.7 $\pm$ 0.3  | 0.79 $\pm$ 0.04 | 0.07 $\pm$ 0.01 | 19.4 $\pm$ 0.7 | Brass                  |        |

\*Influence from internal corrosion as shown in the optical microscopy study (section 3.2.3. Influence of corrosion)

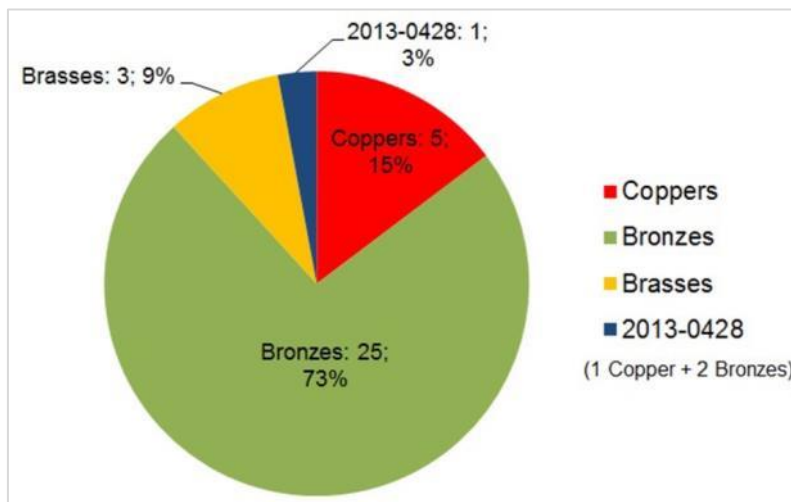


**Figure 7.** Relative frequencies of metal type in the analyzed copper-based artefacts.

Lead contents are always under 0.8% Pb except in one brass ring, the 2013-0442, with 7.2% Pb. The lead contents under 2% are frequently assumed as ore contaminations, being higher values normally related to intentional additions (Figueiredo 2010). The arsenic contents are generally under the quantification limit of 0.1% As, or just above that value, being the little bent copper sheet and the brass capsule those that show the highest values (~0.8% As). Iron is always present under the quantification limit of 0.05% Fe, with the exception of all the brass artefacts (0.07-0.35% Fe) and the copper ring 2013-0434 that has 0.05% Fe. A higher iron content in these artefacts (>0.05%) can be related to a different type of metal production technology, as stronger reduction conditions (Craddock & Meeks 1987), that possibly point out to a different origin or chronology of these artefacts.

On the major group of artefacts, the bronze alloys, the tin contents are mostly between 10 and 15% (the exceptions are one bar with ~5% and one ring with ~8% Sn) (Fig. 8). This alloy composition and the low content of impurities can be related to the bronze compositions from LBA and transition to EIA in the Portuguese territory (Figueiredo *et al.* 2011c; Figueiredo *et al.*, 2013a).

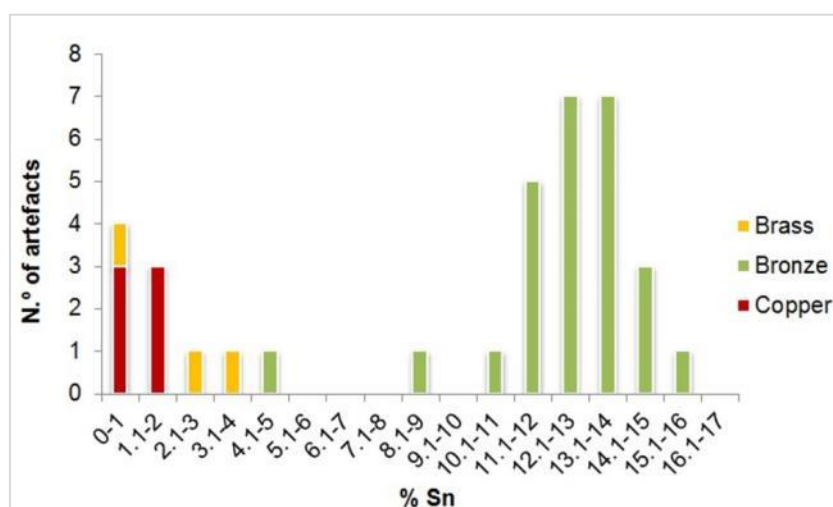


**Figure 8.** Histogram of Sn content in the studied copper-based artefacts.

Also, the current use of these amounts of tin can be related to the awareness and “control” of the physical or aesthetical properties of this type of alloy by the ancient craftsmen. This range in the tin composition offers particular mechanical properties and coloration to the metal. A bronze with >10% Sn can be substantially hardened by solid solution of Sn in Cu- $\alpha$ , becoming much more hard than copper (Lechtman 1996). This higher hardness with the loss of ductility can be recovered by annealing in objects with tin contents below 15% because this is the solubility limit before the formation of a harder phase, the  $\delta$  phase, enriched in Sn (details on phase diagram for bronzes under annealing conditions in Centre Technique des Industries des Alliages Cuivreux 1967). Additionally, a coloration more likely to gold is obtained inside this range of percentages (Fang & McDonnell 2011), being possible that this golden hue could be significant at the time.

The low content of tin (<2% Sn) in some of the copper artefacts (namely, two rings 2013-0434 and 2013-0435, and the bar 2013-0453) can be related to the presence of this element in the original copper ores used to make the metal (Rovira & Montero, 2003), or to the mixing of copper metal with some bronze in a recycling process.

Within artefacts of the same typology, as in the case of the rings, one can find the three types of metallic materials: there are 12 rings made of bronze, 3 made of copper, and 2 made of brass. As it was said before, the rings can be divided in three groups according to their diameter size (see chapter 1.), and it is observed that the larger rings are all made in bronze, the medium ones are made in bronze and copper and the smaller ones are made in bronze and brass. Observations made under naked eye showed no particularity - in respect to cross-section thickness, diameter or surface finishing - that could clearly distinguish the brass rings or the copper rings in respect to the bronze ones. Some similar features were found only among two copper rings, the 2013-0434 and 2013-0435 that could or not be casual. All the rings show corrosion products with a similar appearance that do not either allow to differentiate them, being however relevant to refer that in their original uncorroded state, a visual differentiation would be possible at least between the copper rings and the copper-alloys, because pure copper has a reddish color and the other copper alloys used have a golden hue. The presence of different types of metal/alloys within this typology can be related to different deposition moments, being that bronze and copper was used during all BA and IA, while brasses are generally more related to Roman times, although in the IP these have been occasionally found in Pre-Roman times, namely in Orientalizing contexts, from the VI century onwards (Montero-Ruiz & Perea, 2007). The presence of these particular artefacts will be discussed in more detail in section 3.4.1 – Early brasses: the presence of two rings and a capsule.

Among the collection it is also observed the use of different metal/alloy in a single object, as in the case of the artefact 2013-0428, which revealed to be composed by a wire made in copper and two rings made in bronze (Fig. 9). The choice of these different materials in the same object could possibly be related with mechanical properties, i.e., the copper was used because its malleability allowed to easy obtain a more thin and bent form, or for aesthetic reasons, resulting in one object with chromatic variations.

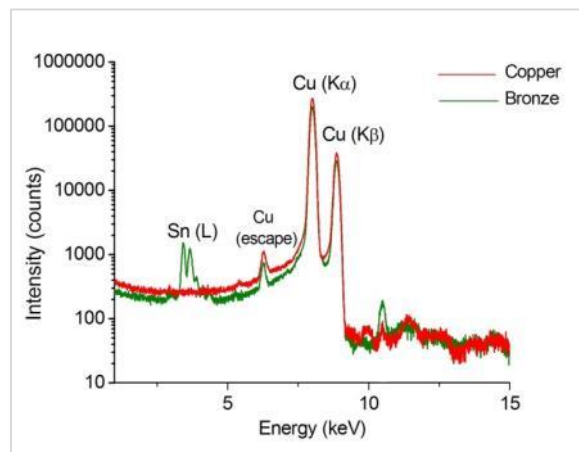


**Figure 9.** Micro-EDXRF spectra of the bent wire (represented in red) and the ring 02 (represented in green) of the artefact 2013-0428.

The thin bent sheet 2013-0456 was manufactured in copper, possibly because of its higher ductility allowing the reduction in thickness.

### 3.2.2 Inclusions in the metallic matrix

The latest studies on archaeological artefacts of the Portuguese territory show that the most common impurities on Proto-historic bronzes are the Cu-S, which according to the Cu-S phase diagram correspond to copper sulfides ( $\text{Cu}_2\text{S}$ ). Other types of inclusions that have also been detected are Sn-O, Cu-S-Fe, Pb, Au and Ag (Figueiredo *et al.* 2011b).

Artefacts of each type of metal/alloy were chosen for SEM-EDS investigations, namely two copper artefacts, two bronzes and the three brasses, taking into account the size of the artefacts due to the equipment restrictions (sample chamber size), and their state of preservation. Table 4 summarizes the type of inclusions observed in each type of artefact.

The inclusions identified in the bronzes were Cu-S and Cu-S-Fe (see Fig. A8 – Appendix V). The Cu-S-Fe inclusions were frequently present inside the Cu-S ones, and could be observed in the backscattered emission mode under a slightly more dark grey tone. This kind of inclusions have previously been detected in LBA and EIA/Orientalizing artefacts and their presence has been related to the use of copper ores with these elements or to specific smelting technologies developed during these periods (Figueiredo *et al.* 2011b).

The analyzed copper artefacts show Cu-S, Sn-O and Cu-S with possibly some Ni-S inclusions (Fig. 10 and Fig. A9 – Appendix V) and one of them, the ring 2013-0434, did also show a Bi-rich metallic inclusion (Fig. 10). The Sn-O inclusions can partially account for the Sn content detected in the micro-EDXRF analysis, and this type of inclusion has previously been found in LBA and EIA/Orientalizing bronze artefacts. The presence of Sn-O inclusions can be related to the partial oxidation of tin during the melting operations (Dungworth 2000) or to non-reacted ore (Klein & Hauptmann 1999). The presence of bismuth has been related with the type/source of the ores used for smelting (Kallithrakas-Kontos *et al.* 2000) and can sometimes be associated to other impurities as arsenic, antimony and nickel (e.g. in an enriched Fahlerz-type ore) (Giumlia-Mair *et al.* 2002). In fact, the ring 2013-0434 (Fig. 10) besides bismuth has nickel rich inclusions, which could be related with the use of a specific type of ore. To mention is that to

present no parallel to this kind of inclusions have been reported for Proto-historic copper or bronze artefacts from the Portuguese territory.

On the brasses (the two rings and the capsule) Zn-S inclusions were observed on all artefacts (Fig. 11), which can be related to the ores used in the metal production, as blende/sphalerite ore (ZnS) (Craddock 1978). The ring 2013-0441 shows Pb metallic inclusions (see Fig.A10 – Appendix IV). In the ring 2013-0442 that has ~7% Pb, this element can be observed as relatively large size globules/grains due to its immiscibility in copper (Scott 1991) (Fig. 11). In the brass capsule (see Fig. A11 – Appendix IV), Bi-Pb metallic inclusions were also observed, being some of them more enriched in Pb and others in Bi. Given the scarcity on studies on Pre-Roman brasses or Roman brasses in the Portuguese territory, no parallels were found for comparison, however, some discussion on these artefacts is presented in section 3.4.1.

**Table 4** Summary of the experimental results relative to the SEM-EDS analysis on the metal inclusions.

| Reference | Artefact | Inclusion              | Metal                 |
|-----------|----------|------------------------|-----------------------|
| 2013-0430 | Ring     | Cu- S / Cu-S-Fe        | Bronze                |
| 2013-0431 | Ring     | Cu- S / Cu-S-Fe        | Bronze                |
| 2013-0434 | Ring     | Cu-S /Ni-S / Bi / Sn-O | Copper                |
| 2013-0435 | Ring     | Cu-S/ Ni-S /Sn-O       | Copper                |
| 2013-0441 | Ring     | Zn-S / Pb              | Brass/Gunmetal        |
| 2013-0442 | Ring     | Zn-S (Pb)              | Brass/Leaded Gunmetal |
| 2013-0457 | Capsule  | Zn-S / Pb-Bi           | Brass                 |

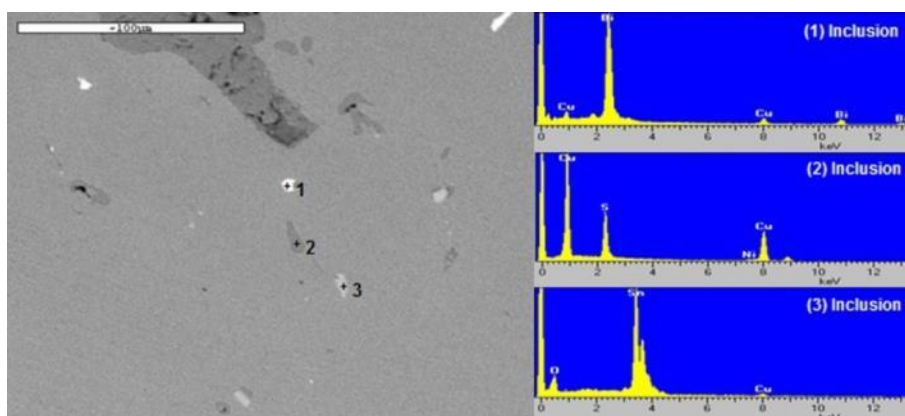


**Figure 10.** SEM (BE) image and spot EDS analysis of the (1) Bi inclusion, (2) Ni-S inclusion and (3) Sn-O inclusion on the copper ring 2013-0434.

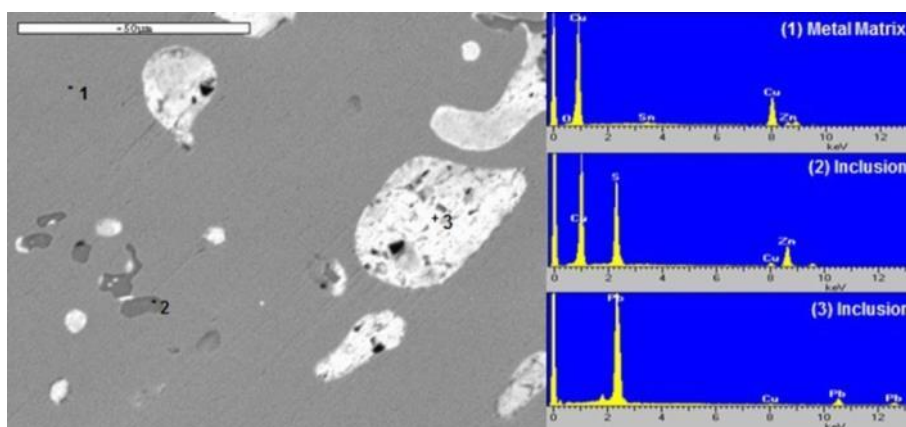


**Figure 11.** SEM (BE) image and spot EDS analysis of the (1) metal matrix, (2) Zn-S inclusion and (3) globules of Pb on the brass ring 2013-0442.

### 3.2.3. Influence of corrosion

As it was said before, the copper-based artefacts that remain under burial environments for long periods of time suffer several physical and chemical transformations involving complex corrosion phenomena that modify the surface of the alloys (Sandu *et al.* 2012).

In the case of bronzes, the corrosion layer can be enriched by alloying elements, like tin, due to the preferential leaching of the copper (decuprification) (Robbiola *et al.* 1998) that results in tin contents measurements superior to the original alloy. The decuprification phenomenon is deeply connected to the presence of the solid  $\alpha$ -phase (Robbiola *et al.* 1998). Tin is the less noble component of the alloy and oxidizes first creating a passivation layer of tin oxide. The diffusion and dissolution of the copper through this oxide layer is associated with the oxygen diffusion towards the interface of the alloy and the oxide, provoking the formation of the corrosion layers (Mabille *et al.* 2003). The quantity of copper ions released is related to the corrosion context, which in the case of archaeological artefacts is the soil, and the individual characteristics of the alloy (Piccardo *et al.* 2007). In Table 5 an example of this phenomenon is shown with the analysis of the ring 2013-0438 over metal and over corrosion.

There is also a process of selective dissolution in the brasses, however, instead of a preferential loss in copper there is a preferential loss in zinc, named dezincification (Stillwell & Turnipseed 1934). In this process of selective corrosion, the Zn in the alloy is preferentially corroded and leached from the alloy, resulting in lower amounts of this element in the corrosion products and in the metal under the corrosion products layer comparing to the bulk alloy composition. This is observed in the brasses of the collection (the capsule and the two rings), as we can see in Table 5.

In unalloyed coppers there can be an enrichment of the minor elements in the superficial corrosion layers when compared to the metal bulk, as present in Table 4 for the copper ring 2013-0437 that shows an increase in As and Fe, being the increase in Fe also a likely consequence of soil contamination during burial (Robbiola 1998).

In general, it can be observed that all the artefacts present an increase of the Sn, As and Pb contents in the corrosion layers when compared to the metal bulks due to decuprification or dezincification phenomenon and an increase in Fe most likely due to soil contamination.

**Table 5.** Summary of the experimental results relative to the corrosion influence on the different type of alloys.

| Reference | Artefact |                | micro-EDXRF (wt. %) |          |          |           |           |          | Metal          |
|-----------|----------|----------------|---------------------|----------|----------|-----------|-----------|----------|----------------|
|           |          |                | Cu                  | Sn       | Pb       | As        | Fe        | Zn       |                |
| 2013-0438 | Ring     | Metal          | 85.2±0.9            | 14.6±0.9 | n.d.     | 0.13±0.01 | <0.05     | n.d.     | Bronze         |
|           |          | over corrosion | 32.9±0.7            | 59.5±5.8 | n.d.     | 0.6±0.1   | 7.1±6.3   | n.d.     |                |
| 2013-0437 | Ring     | Metal          | 99.9±0.0            | n.d.     | n.d.     | <0.10     | <0.05     | n.d.     | Copper         |
|           |          | over corrosion | 97.3±0.1            | n.d.     | n.d.     | 0.31±0.03 | 2.4±0.1   | n.d.     |                |
| 2013-0441 | Ring     | Metal          | 82.0±1.0            | 2.9±0.1  | 0.3±0.1  | 0.03±0.1  | 0.35±0.01 | 14.5±1.0 | Brass/Gunmetal |
|           |          | over corrosion | 81.0±0.6            | 3.8±0.5  | 5.8±0.2  | 0.4±0.1   | 6.3±0.2   | 2.9±0.1  |                |
| 2013-0442 | Ring     | Metal          | 79.7±3.2            | 3.5±0.5  | 7.2±2.8  | <0.10     | 0.28±0.02 | 9.1±0.7  | Brass/Gunmetal |
|           |          | over corrosion | 52.5±7.0            | 25.5±3.2 | 15.5±3.0 | 0.5±0.4   | 2.9±0.5   | 3.0±1.6  |                |
| 2013-0457 | Capsule  | Metal          | 79.0±1.0            | n.d.     | 0.7±0.3  | 0.79±0.04 | 0.07±0.01 | 19.4±0.7 | Brass          |
|           |          | over corrosion | 96.0±0.6            | 0.7±0.7  | 0.3±0.06 | 0.3±0.04  | 0.1±0.03  | 2.4±0.3  |                |

### 3.3.1. Manufacturing techniques

The OM allowed the observation of some common features within the metallic collection. The most regular characteristics found among the artefacts were equiaxial  $\alpha$  grains with annealing twins. This features appear after heating (recrystallization annealing) a cold worked metal (plastic deformation at low temperatures, generally by hammering) to recover its ductility. In some artefacts the grains did also show slip bands, which are related to cold deformation with absence of a subsequent annealing. The presence of slip bands can be due to use of the artefact provoking some plastic deformation, its break, or can indicate that the operation sequence was finished with cold work, as hammering, or a final surface polishing (Wang and Ottaway, 2004), whose intensity can be related with the density of the lines. The presence of artefacts with as-cast microstructures (not presenting the previous features and alternatively exhibiting a dendrite grain structure or cored grains) was detected among various typologies but was not as frequent.

Besides the presence of the  $\alpha$  (copper rich) phase, it was also possible to observe the presence of a blue-silver form in some of the bronze artefacts, that is the  $\delta$  phase rich in tin (as confirmed by SEM-EDS analysis), part of the ( $\alpha+\delta$ ) eutectoid (Fig. 12 A) (Cu-Sn phase diagrams in Fig. A4 and A5 Appendix II). This eutectoid is generally present along the  $\alpha$ -copper grain boundaries (as in interdendritic regions in as-cast alloys), and its presence in some artefacts can be related to low thermo-mechanical sequences in homogenizing the alloy (insufficient homogenization of the alloy during annealing operations).

The dark grey inclusions that were analyzed by SEM-EDS (see section 3.2.2) and identified as Cu-S, are sometimes elongated perpendicularly to the hammering direction of the artefact evidencing a high deformation applied on certain artefacts in the process of shaping (Fig. 12 B). This implies an operational sequence that comprises several forging and annealing cycles. Inside some of them it was possible to observe another darker colored inclusion of smaller size (Fig. 12 C), that accordingly to the SEM-EDS could be Cu-S-Fe or Sn-O in the bronze or copper artefacts with low tin contents.



**Figure 12.** Microstructure of the ring 2013-0439 (A), the bar 2013-0453 (B) and the rivet 2013-0450 (C) (OM) showing ( $\alpha+\delta$ ) eutectoid, Cu-S inclusions among the  $\alpha$  copper phase and dark colored inclusion inside the Cu-S inclusion.

A summary of the results from the OM observations are presented in Appendix III, with the individual manufacturing processes annotated for each artefact and the Sn content of each artefact also shown since, together with the manufacturing process, it can influence the presence or absence of the eutectoid in the bronzes.

In Fig. 13 the type of thermo-mechanical processing determined for each group of artefacts is presented, and it is possible to see that the majority of the artefacts suffered thermo-mechanical sequences (with forging and deformation cycles), being the group composed by bars and rings (Others) the one that presents a higher variety in the type of thermo-mechanical processing.

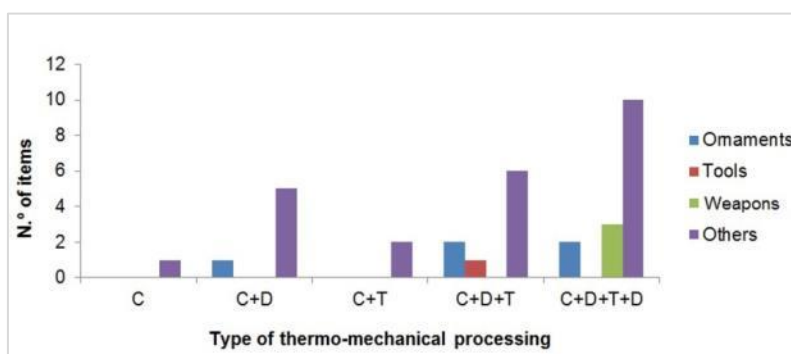


**Figure 13.** Type of thermo-mechanical processing in the studied copper based artefacts.

In the next subsections detailed descriptions of some of the artefacts microstructure and manufacturing processes are made accordingly to each group (weapons, ornaments, tools and others – bars and rings).

### 3.3.1.1. Weapons

In the dagger 2013-0423 it's possible to visualize in the central rib the presence of its as-cast microstructure, with many thin dendrites, evidenced by corrosion (Fig. 14). This is very different of the microstructure observed in the blade and in the top of the handle which show recrystallized grains, suggesting that after casting the object was only worked on the edges and not in the center. This differential processing can be related to the final shaping and sharpening of the blade, since the blade needs to be thin and possibly harder. The dagger 2013-0424 presents a microstructure that resulted from cycles of forging and annealing at the center and edge of the blade, and the top zone of the handle does also show the presence of slip bands (Fig. 14) that could have resulted from some deformation due to the break of the handle or related to some finishing operation to fit the hilt. These slip bands are also seen at the top zone of the handle of the dagger 2013-0425 (Fig. 14).

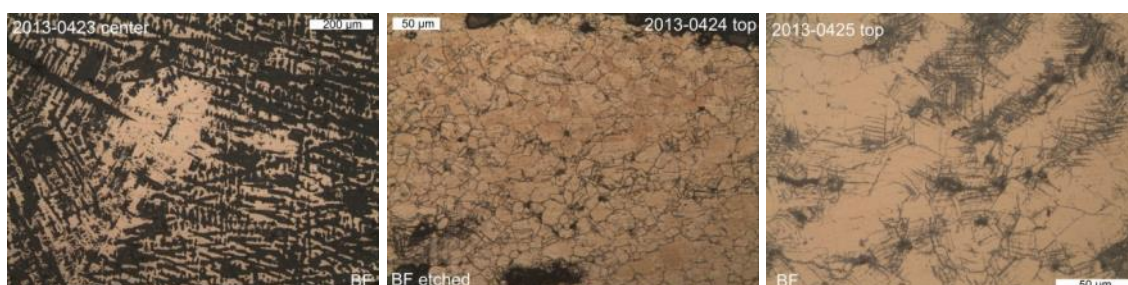


**Figure 14.** Microstructure of the daggers 2013-0423, 2013-0424 and 2013-0425 (OM).

### 3.3.1.2. Ornaments

In the nail 2013-0447 both parts of the artefact – the head and the pin – present recrystallized grains with annealing twins but the pin shows a high amounts of slip bands (Fig. 15). This suggests that after casting and annealing the object suffered a final cold deformation, which could be related to the shaping of the pin into a near-quadrangular cross-section or to the process of fixing the nail to some base object.

The head of the pendant 2013-0448 presents a dendritic microstructure homogenized by an annealing treatment. However, this annealing was not sufficient to cause recrystallization of the grain structure (Fig. 15). The microstructure of the pin revealed recrystallized grains with annealing twins and some slip bands, evidencing a thermo-mechanical sequence of forging and annealing and possibly a surface finishing (Fig. 15). In the pendant 2013-0449 it's possible to see an as-cast microstructure, with coarse dendrites in the head, as well as some superficial deformations (slip bands), and the pin has a dendritic structure also with some evidences of superficial deformations. These microstructures confirm that this kind of object was shaped in a mould and suffered posterior minor works, either for shape corrections or surface final treatment (Fig. 15), and are also in agreement with the radiographic images (section 3.1.) that suggest that they are compact objects. Possibly, the differences between head and pin in the latest pendant (2013-0449) can be related with different cooling rates, having the head cooled slower and thus developed coarser grain structure.

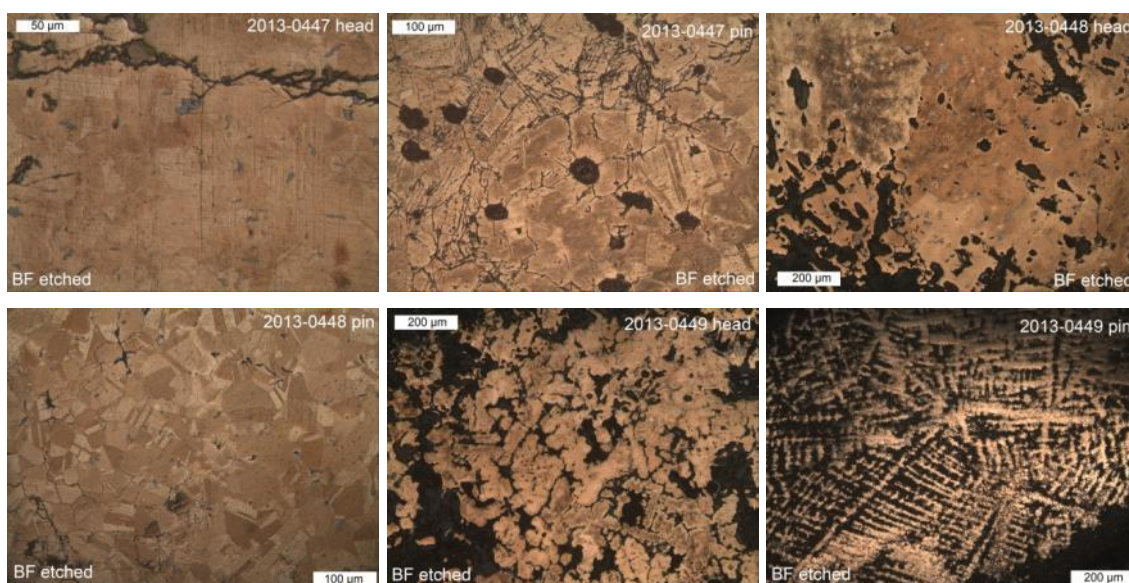


**Figure 15.** Microstructure of the nail 2013-0447, the pendant 2013-0448 and the pendant 2013-0449 (OM).

### 3.1.1.3. Tools

The tranchet 2013-0426 presents a microstructure with clear recrystallized grains and annealing twins in the entire artefact except the top zone of the blade (Fig. 16 A) previously depicted at the digital radiography of the object (see section 3.1), where larger sized grains are present. This feature shows that this region of the artefact was probably less worked than the lower edge (Fig. 16 B), possibly with some consequence in the development of the corrosion in this area.

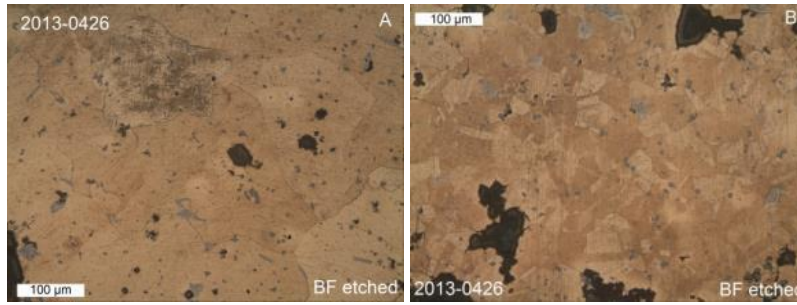


**Figure 16.** Microstructure of the tranchet 2013-0426 (OM).

#### 3.1.1.4. Others – bars and rings

All the bars present a recrystallized grain microstructure with annealing twins except the bronze bar 2013-0455, that present large sized grains, in a coarse dendritic shape, with some slip bands, suggesting that this object obtained its shape in the mould and possibly only some posterior surface deformation was applied (see bar 2013-0455 in Fig. A7 – Appendix IV).

In the typology of the rings (Fig. 17) it was possible to see that the bigger and thinner rings (from 2013-0429 to 2013-0439) have more evidences of the application of thermo-mechanical sequences in their manufacture (see ring 2013-0431 in Fig. A7 – Appendix IV), i.e., they were more worked, than the smaller rings (from 2013-0440 to 2013-0445) that seem to have been only slightly worked (see ring 2013-0442 in Fig. A7 – Appendix IV). In the middle sized group rings the copper rings (2013-0434, 2013-0435 and 2013-0437) show much less or almost none evidence of thermo-mechanical processing, being possibly related to the ductility of copper in relation to bronze that is easily work hardened (see 2013-0437 in Fig.A7 – Appendix IV).

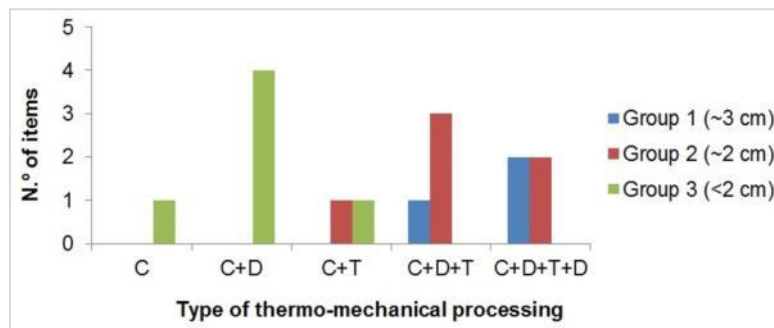


**Figure 17.** Type of thermo-mechanical processing in the typology of the rings.

The small size bronze rings 2013-0444 and 2013-0445 have a dendritic structure (see Fig. A7 – Appendix IV) and both show evidences of having been cast in a bivalve mould (two piece mould) due to the presence of a casting seam in the interior of the rings, showing that they didn't had an extreme finishing procedure after casting. The ring 2013-0444 does also have two irregular external surfaces in opposed sides to each other, suggesting the location of channels through which the metal was poured into the mould. For the present case it could also be suggested that the mould used for producing the rings could possibly make various rings, as it was represented on a scheme for Medronhal rings (Figueiredo 2010).

### 3.3.2. Intergranular corrosion

In many of the small polished surfaces intergranular corrosion was observed at the edges of the prepared areas (representing an area more near to the corroded surface) (Fig. 18 A). In some cases, intergranular corrosion developed deeply, and the superficial polishing did not allow obtaining an area free of corrosion. Consequences to this was observed in the micro-EDXRF analyses (see Table 3 in section 3.2.1.) were some of the analyses made on some parts of the objects, as the dagger 2013-0423, show higher tin contents, different from the totally uncorroded metal, and which are related to the corrosion processes reported on section 3.2.3.

In some microstructures it was possible to visualize metallic copper (appearing as pink areas under BF, OM) in regions affected by corrosion (Fig. 18 B). Generally, this copper has irregular shapes and seems to be filling previous empty spaces, as pores, or is present among the intergranular corrosion in long and thin shapes. It's a result of a process of selective corrosion (Wang & Merkel 2001) and according to Tylecote (1979), there's a temporary dissolution of both constituents of the binary alloy and consequent redeposition of copper due to the further dissolution of tin (destannification). This redeposition occurs at the internal regions where oxygen concentration is low. Also, this feature is commonly found in archaeological bronze alloys being usually used as an indicator of long term corrosion (Bosi *et al.* 2002).

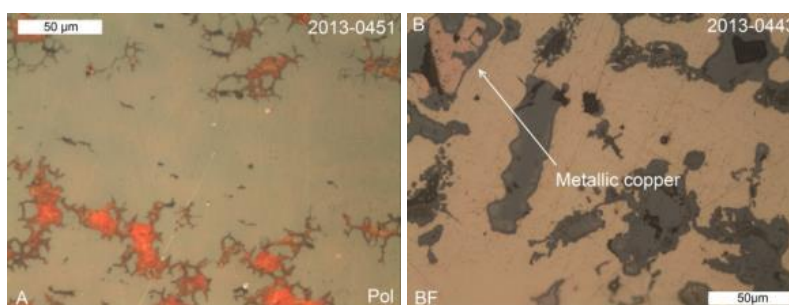


**Figure 18.** Microstructure of the bar 2013-0451 with intergranular corrosion and the ring 2013-0443 with metallic copper.

### 3.4. Some specificities of the collection

#### 3.4.1. Early Brasses: the presence of two brass rings and a capsule

The appearing of the two rings and the capsule made in a copper alloy with relatively high amounts of Zn is a particularity that is worth highlighting in the present work because before and even during the Roman period little is known about the use and/or the production of brass in the IP. In addition to this, still much is unknown related to the evolution of the trade with the Eastern Mediterranean through the colonization of the IP by the Phoenicians and the Greeks that could have transferred new materials and technologies (Montero-Ruiz & Perea 2007). The presence of brasses in the IP during Proto-history is known from at least the VI century BC onwards, being the earliest object (a pin from Casa del Obispo, Spain) found in a colonial/Orientalizing context of the VI century BC, being other objects (a needle, two sheets and a rod) found in IA cultural contexts of the IV-III century BC. These objects have been explained as importations from the Eastern Mediterranean, and other objects detected with lower and variable contents of Zn have been proposed to possibly have been manufactured with mixtures of metals, including

exogenous material/brasses that did already circulated as recycled metal (Montero-Ruiz & Perea 2007).

Zinc is highly reactive and do not occur as a native metal, being its ores normally related with other metals as lead in Antiquity deposits. Its high volatility at c. 907° C, above which it only exists as a vapour, constitutes a problem in the brass production (Craddock 1990, Rehren & Martín-Torres 2008). It is known that in Antiquity, a certain copper ore rich in zinc from Eastern Mediterranean (a rock near Andeira, Northwest Asia Minor) was treated in a furnace to produce some droplets of “false silver” (metallic zinc that was condensed in the cooler parts of the furnace) and was added to copper to produce *oreichalkos*, known as the copper of the mountains (Bayley 1990, Thornton & Ehlers 2003). The obtained alloy was considered rare and expensive (Craddock 1990) and the majority of zinc was vaporized during the process resulting in low contents of Zn in the alloy (Bayley 1990).

It is believed that the metalworkers at the time were not aware of the zinc content or were not in possession of the technical knowledge to control it. It was not until much later in the history, with the development of more complex processes that also could allow the mass-production of brass, as the cementation process used by the Romans in the I century BC, that some control in the alloy was possible (Thornton & Ehlers 2003, Craddock 1990). The cementation process involved a closed crucible where metallic copper, charcoal and powdered zinc ore were heated together (to force the reaction and not let the vapors escape with the furnace gases) so that the zinc vapours could react with the metallic copper, being absorbed into the solid copper solution, producing brass with high zinc contents (Rehren & Martín-Torres 2008). The Zn contents in this kind of alloy production are over 20% Zn (Bayley 1990), but during the melting of fresh cementation brass foregone casting this content can drop frequently to contents around 18% Zn due to the loss of volatile Zn (Dungworth 1997).

Brasses can be classified as gunmetal when copper is alloyed with several percent of both zinc and tin, and as leaded gunmetal when lead is also added to the alloy (over about 4%) (Bayley 1990). These alloys can be a result of mixing scrap metals of different compositions, as bronzes with brasses (Dungworth 1997).

In the present collection, the two rings 0441 and 0442 have 14.5 and 9.1% Zn and some tin (2.9-3.5% Sn) that could classify them as gunmetals or leaded gunmetal in the case of the ring 0442 (7.2% Pb). On the other hand, the capsule has a higher amount of zinc (19.4% Zn) but has only vestiges of lead (0.7% Pb) and no evidences of tin.

In the table shown in Figure 19 the composition of the brasses from MG is compared with other early brasses from different regions and periods. A relatively wide dispersion among the Zn, Pb and Sn contents is observed among all the groups, being however relevant to observe that the later brasses (the brooches from I century AD) tend to have higher Zn contents and relatively low Sn and Pb contents, a tendency also found in the capsule of the MG artefact. The earliest brasses, the two XIII century rings from Eastern Mediterranean have very different compositions, with variations in Zn, Sn and Pb. The early brasses found in the Southern and Eastern IP (Spain) do also show a great variability in the Zn and Pb contents, nevertheless with a tendency to lower variability and amounts in the Sn content.

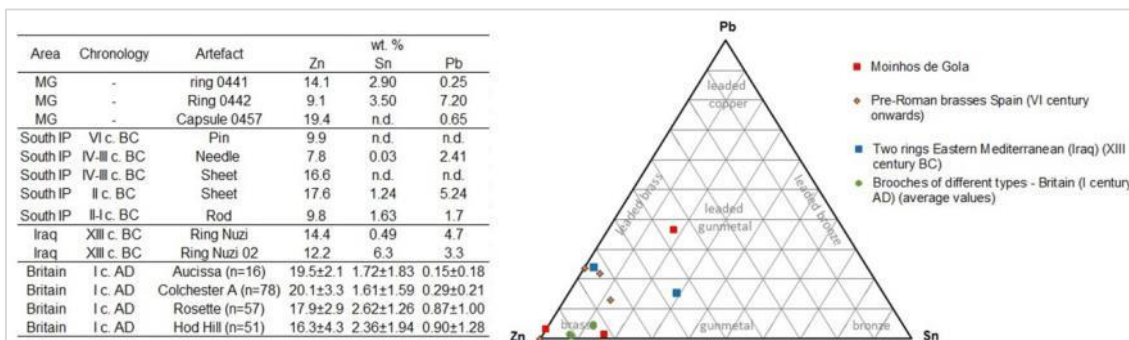


**Figure 19.** Table with Zn, Sn and Pb contents of brass objects from Moinhos de Gola and other early brasses from Spain, Eastern Mediterranean and Britain (Montero-Ruiz & Perea 2007 and Bayley 1990) and a ternary diagram considering these elements normalized to 100%.

Taking into consideration this preliminary discussion, it can be proposed that the MG brass artefacts could be imported objects or objects of later periods, such as Roman. The latest would be a hypothesis especially adequate for the capsule, since it is rather higher zinc content (19.4% Zn) and its absence or low content in Sn and Pb, suggests brass production by the cementation process.

In relation to the capsule 2013-0457, an object of a similar shape and size was found in the late sixties of the XX century in Casa da Orca da Cunha-Baixa, a passage grave in Central Portugal with an initial occupation attributed to the initial stage of the megalithic phenomena of the region (Castro Nunes *et al.* 1989), being this object clearly assumed as a later addition, probably from the LBA. It was given a decorative function to it, but the absence of a fixation element in its internal concave surface showed that it was not functionally equivalent to the nails and buttons widely known in the LBA contexts. The lack of direct parallels leads to the assumption that the artefact could be a sheath probe or a hilt ornament of a dagger (Castro Nunes *et al.* 1989).

Elemental analysis was made on that artefact, however these were only made over the corrosion products and thus cannot be taken into account to a rigorous classification of the alloy used because of the corrosion phenomena described before (see section 3.2.3.). However, comparing the analysis made on the MG capsule over the corrosion products to the ones made on the artefact from Casa da Orca, it can be observed that the major elements that compose a brass – Cu and Zn – are present in very similar contents (Table 6). This may suggest that the artefact found in Casa da Orca was also made of brass, providing an important parallel to the MG capsule. Next, an additional study on this artefact is being presented, which can contribute to the understanding of the fixing system of this kind of objects.

**Table 6.** Results of elemental analysis performed over corrosion on the artefact found in Casa da Orca (Castro Nunes *et al.* 1989) and the capsule found in the present collection.

| Reference | Artefact              | %        |         |         |          |          |          |            |          |            |  |
|-----------|-----------------------|----------|---------|---------|----------|----------|----------|------------|----------|------------|--|
|           |                       | Cu       | Zn      | Sn      | As       | Fe       | Pb       | Ni         | Ag       | Sb         |  |
|           | Casa da Orca artefact | 93±1.0   | 2.6±0.7 | 0.2±0.1 | 1.4±0.4  | 2.6±0.3  | -        | -          | 0.1±0.02 | 0.04±0.005 |  |
| 2013-0457 | Capsule               | 96.0±0.6 | 2.4±0.3 | 0.7±0.7 | 0.3±0.04 | 0.1±0.03 | 0.3±0.06 | 0.08±0.003 | -        | -          |  |

### 3.4.2. Joining metals in Antiquity: the case-study of the capsule

The capsule, besides having been manufactured in brass, also has another particularity discovered during the archaeometallurgical study that gives further clues to the observations

made in the 1980's on the Casa da Orca similar object. After the observation of the radiographic images, it was possible to observe a dark spot area (see Fig. 6 in section 3.1.), that with a more detailed observation under naked eye correspond to a small sized material ( $\sim 1 \text{ mm}^2$ ) over the corrosion products on the exterior of the capsule, with different coloration (a silvery color, after a gentle superficial cleaning) of the corrosion products of the surrounding area (that are from brown to dark brown) (Fig. 20). Superficial micro-EDXRF analysis made on this small sized material revealed that it is composed by a copper-tin alloy (Table 7) with a low amount of Pb and As, and the presence of some Zn (the presence of some internal corrosion may have risen the Sn content and lowered the Zn relatively to the original one - see SEM-EDS microstructure in Fig. 21 and section 3.2.3.).

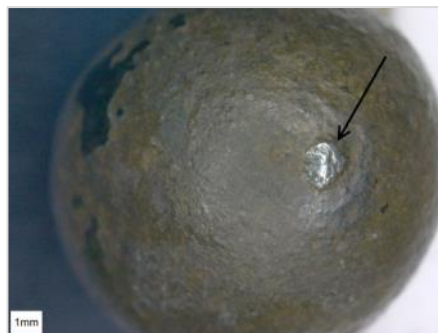


**Figure 20.** Superficial spot material over the corrosion products on the exterior of the capsule 2013-0457 by stereomicroscope (10x).

**Table 7.** Results of micro-EDXRF analyses made over the superficial spot material on base metal and corrosion of the capsule 2013-0457.

| Reference | Artefact                    | micro-EDXRF (wt. %) |          |         |         |           |           |            |          |
|-----------|-----------------------------|---------------------|----------|---------|---------|-----------|-----------|------------|----------|
|           |                             | Cu                  | Sn       | Pb      | As      | Fe        | Ni        | Zn         |          |
| 2013-0457 | Superficial spot material * | 64.9±5.0            | 30.8±4.1 | 0.7±0.7 | 1.0±0.3 | 0.20±0.20 | 0.11±0.00 | 2.24±0.25  |          |
| 2013-0457 | Capsule                     | Metal               | 79.0±1.0 | n.d.    | 0.7±0.3 | 0.8±0.04  | 0.07±0.01 | 0.08±0.01  | 19.4±0.7 |
|           |                             | over corrosion      | 96.0±0.6 | 0.7±0.7 | 0.3±0.1 | 0.3±0.04  | 0.1±0.03  | 0.08±0.003 | 2.4±0.3  |

\*Influence of the preferential corrosion of the  $\alpha$ -phase.

This capsule could have been a decorative element, as suggested in the study of the similar object found in the sixties (Castro Nunes *et al.* 1989), and this superficial spot material could be what was left from a joining element to attach it to another object, as a dagger hilt, a necklace or a bracelet, to adorn it. The joining to the other object would have been made in the outer convex surface of the capsule, supporting the observations made by Castro Nunes *et al.* (1989) of the lack of a joining system in the internal concave surface of the capsule of Casa da Orca.

A joining process can be made by mechanical means (e.g. riveting), a casting-on technique (as casting one part of an artefact directly over another pre-existent part) or, given the small size of the material on the surface and its apparently high adherence to the base metal, another process can be considered as a possibility in the present study, which is soldering.

There are two types of soldering: soft soldering, that is the joining of metals by means of a low melting temperature alloy, usually lead and/or tin, with the union being made without fusing of the parent metal or apparent alloying, and hard soldering, or brazing, that is a process in which molten metal of a composition with a melting temperature lower than that of the parent metal is used to fill/bridge a very narrow space between them. Hard soldering needs a skillful worker and can occur at temperatures  $\sim 550^\circ\text{C}$  up to  $850^\circ\text{C}$ , and the soldering results in very strong joints (Coghlan 1975).

Taking into account the elemental analysis of the superficial spot material, which shows that it is made of a Cu-Sn alloy, and the presence of some Zn that is incorporated in the alpha phase (Fig. 21), if soldering had been performed in this artefact, then it can be suggested that it was

hard soldering, since a Cu-Sn alloy has a relatively high melting temperature (see Cu-Sn phase-diagram Fig. A4 and A5 – Appendix II), and the presence of Zn could be understood as partial melting of the base metal with some diffusion/alloying occurring during the process (see Cu-Zn phase-diagram Fig. A6 – Appendix II). Although the scarce evidences for the use of Cu-Sn alloys as solders, Maryon (1949) refers copper-tin as an hard solder used in Antiquity for copper, bronze or brass artefacts, providing some further leads to the hypothesis of this superficial spot material being a soldering element.

Despite the fact that it is not possible to clearly know the exact contents of copper and zinc in the solder by the analysis made because of the influence of the corrosion, the present case-study brings novel and interesting information, and points out that further studies should be considered on the artefact<sup>3</sup>.

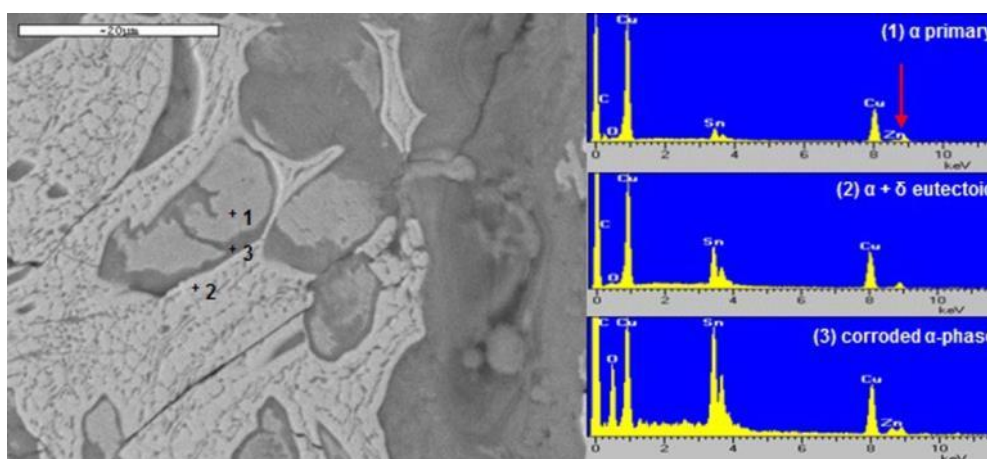


**Figure 21.** SEM (BE) image and spot EDS analysis of the (1) remain of  $\alpha$  primary grain, (2)  $\alpha + \delta$  eutectoid and (3) corroded  $\alpha$ -phase on the superficial spot material on base metal of the capsule 2013-0457.

#### 4. Conclusions

The present investigation revealed very interesting details of the archaeological artefact collection, clearly bringing new emphasis and conferring possible new meanings to the collection when compared to the preliminary study performed earlier.

The application of the X-ray radiography, the observation by stereomicroscope, the micro-EDXRF and SEM-EDS analyses as well as the OM observations revealed to be suitable in order to obtain complementary and appropriate information about the preservation state, the composition and the manufacture techniques of the metallic artefacts.

The X-ray radiography revealed to be a great tool to the evaluation of the conservation state of some particular objects within the collection, revealing features as structural heterogeneities that were frequently related to localized corrosion/degradation processes, and also some fissures and fractures which could possibly be related to use, as in the daggers. These features are not all visible by naked eye, but can have implication in the handling of the objects and in their conservation state.

<sup>3</sup> To present, transmitted X-ray diffraction by synchrotron radiation (in HEMS Beam Line at Petra III, Hamburg, Germany) was made on the area but results revealed to be much influenced by the superficial corrosion. Possibly, X-ray micro-tomography could be applied to study this particular region in a near future.

The micro-EDXRF analyses allowed the classification of the type of metal/alloys of each artefact as well as the study of some corrosion phenomena present in each type of alloy. It was possible to show that the majority of the artefacts were made of binary bronze (73%), reveal the presence of a number of copper artefacts (15%) and that three objects were made of brass (9%). The results revealed a certain compositional variety within each type of alloy, particularly among the brasses, that showed varied contents of Zn, Sn and Pb, which could designate one of them as a gunmetal and another one as a leaded gunmetal. The majority of the bronze artefacts have Sn contents between 10 and 15% and low amounts of impurities, which can generally relate them with the LBA or EIA metallurgy of the Portuguese territory.

It was also observed the association of different metals/alloys within two objects – a copper wire with two bronze rings and a brass capsule with a small superficial bronze material that could possibly be a solder – and within the same typology of artefacts – the ring typology, with rings made of bronze, of copper or brass.

The OM observations allowed to infer about the manufacturing processes revealing that the majority of the artefacts of the collection suffered thermo-mechanical cycles, which in some artefacts, such as daggers, could be more intense in the blade areas and among the rings could be more intense in the larger sized rings that did also presented a thinner cross-section.

The inclusions identified in the metallic matrixes of the artefacts showed a rather great variability, especially among the different types of metal/alloys. Besides the Cu-S inclusions, that are common to bronzes and coppers, some bronzes also have Cu-S-Fe inclusions, some coppers have Sn-O inclusions and brasses have Zn-S inclusions. Bismuth and bismuth-rich inclusions (associated with lead) were also found in one copper ring and in the brass capsule, respectively, and this type of inclusion had not been observe before in LBA/EIA copper or bronzes from the Portuguese territory. The presence of these inclusions/elements can be related to the use of a specific ore for the metal production.

The presence of brasses provides some singularity to the collection due to the scarcity of information about this kind of alloys in Pre-Roman times and the lack of archaeometallurgical studies in Roman brasses at the IP. Their presence can be interpreted as importations related to the circulation of exogenous products during the Proto-history and/or to the deposition of materials during different moments at the site, namely during the transition of LBA/EIA (Orientalizing period) onwards, including during the Roman period. The relatively high zinc content and absence or small amounts of tin and lead in the capsule in relation to the two rings, could possibly relate it to a specific process of brass production, as the cementation process, used during Roman times.

## References

- Araújo, M.F., Barros, L., Teixeira, A.C., Melo, A.A. 2004. EDXRF study of prehistoric artefacts from Quinta do Almaraz (Cacilhas, Portugal). *Nucl Inst Meth B* (1): 741-746.
- Araújo, M.F., Silva, R.J.C., Senna-Martinez *et al.* 2013. Investigação em Arqueometalurgia em Portugal, resultados recentes e perspectivas futuras de uma equipa multidisciplinar. *Almadan II*, 17: 69-78.
- Arruda, A. M. 2008. Fenícios e púnicos em Portugal: problemas e perspectivas. *Cuadernos de Arqueología Mediterránea*, 18: 13-23. Barcelona: Universidad Pompeu Fabra.
- Bayley, J. 1990. The production of brass in Antiquity with particular reference to Roman Britain. *2000 years of zinc and brass*, number 50: 7-23.
- Bosi, C., Garagnani, G.L., Imbeni, V. *et al.* 2002. Unalloyed copper inclusions in ancient bronze artefacts. *J Mater Sci* 37, 4285-4298.
- Bronk, H., Röhrs, S.; Bjeoumikhov, A; *et al.* 2001. ArtTAX – a new mobile spectrometer for energy-dispersive micro X-ray fluorescence spectrometry on art and archaeological objects. *Fresen J Anal Chem*, 371: 307-316.
- Canha, A., Valério, P., Araújo, M.F. 2007. Testemunhos de metalurgia no povoado de Canedotes (Bronze Final). *Revista Portuguesa de Arqueologia*, 10: 159-178.
- Castro Nunes, J., Bragança Gil, F., Senna-Martinez, J.C., Guerra, F. 1989. Artefacto metálico recolhido na Casa da Orca da Cunha Baixa, concelho de Mangualde. *Actas do I Colóquio Arqueológico de Viseu*: 61-63.
- Centre for Archaeology Guidelines. 2001. *Archaeometalurgy*. English Heritage.
- Centre Technique des Industries des Alliages Cuivreux. 1967. *Atlas Metallographique des Alliages Cuivreux*. Paris: Éditions Techniques des Industries de la Fonderie.
- Craddock, P.T. 1978. The composition of the copper alloys used by the Greek, Etruscan and Roman civilizations – 3 The origins and Early use of brass. *J Archaeol Sci*, 5: 1-16.
- Craddock, P.T., Meeks, N.D. 1987. Iron in ancient copper. *Archaeometry* 29: 187-204.
- Craddock, P.T. 1990. Zinc in Classical Antiquity. *2000 years of zinc and brass*, number 50: 1-6.
- Craddock, P.T. 1995. *Early metal mining and production*. The University Press, Cambridge.
- Coghlan, H.H. 1975. *Notes on the metallurgy of copper and bronze in the Old World*. The University Press, Oxford.
- Dungworth, D. 1997. Roman Copper Alloys: Analysis of Artefacts from Northern Britain. *J Archaeol Sci* 24: 901-910.
- Dungworth, D. 2000. Serendipity in the foundry? Tin oxide inclusions in copper and copper alloys as an indicator of production process. *Bulletin of the Metals Museum*, 32: 1-5.
- Fang, J., McDonnell, G. 2011. The colour of copper alloys. *The Journal of the Historical Metallurgy Society*, 45 Part 1: 52-61.
- Figueiredo, E., Melo, A.Á., Araújo, M.F. 2007. Artefactos metálicos do Castro de Pragança: um estudo preliminar de algumas ligas de cobre por espectrometria de fluorescência de raios X. *O Arqueólogo Português*, 25: 195-215.
- Figueiredo, E. 2010. *A study on metallurgy and corrosion of ancient copper-based artefacts from the Portuguese territory*. Tese de Doutoramento. Universidade Nova de Lisboa.

- Figueiredo, E., Araújo, M.F., Silva, R.J. *et al.* 2011a. Characterisation of Late Bronze Age large size shield nails by EDXRF, micro-EDXRF and X-ray digital radiography. *Appl Radiat Isotopes*, 69: 1205-1211.
- Figueiredo, E., Valério, P., Araújo, M.F. *et al.* 2011b. Inclusions and metal composition of ancient copper-based artefacts: a diachronic view by micro-EDXRF and SEM-EDS. *X-Ray Spectrom*, 40 : 325-332.
- Figueiredo, E., Silva, R.J.C., Braz Fernandes, F.M. *et al.* 2011c. Smelting and recycling evidences from the Late Bronze Age habitat site of Baiões (Viseu, Portugal). *J Archaeol Sci*, 37: 1623-1634.
- Figueiredo, E., Lopes, F., Araújo, M.F. *et al.* 2012. Os primeiros bronzes do território português: uma primeira abordagem arqueometalúrgica a um conjunto de machados tipo bujões/Barcelos. *Estudos Arqueológicos de Oeiras*, 19: 71-78.
- Figueiredo, E., Araújo, M.F., Silva, R.J.C., Vilaça, R. 2013a. Characterisation of a Proto-historic bronze collection by micro-EDXRF. *Nucl Inst Meth B*, 296: 26-31.
- Figueiredo, E., Silva, R.J.C., Araújo, M.F. & Fernandes, F.M.B. 2013b. Multifocus Optical – microscopy Applied to the Study of Archaeological Metals. *Microsc Microanal*, 19: 1248-1254.
- Fonte, J., Bettencourt, A.M.S., Figueiredo, E. 2013. Deposições Metálicas do Bronze Final no Vale do Assueira. O Caso do Sítio de Moinhos de Golas (Solveira, Montalegre, Norte de Portugal). *Estudos do Quaternário*, 9: 17-27.
- Giumlia-Mair, A., Keall, E.J., Shugar, A.N., Stock, S. 2002. Investigation of a Copper-based Hoard from the Megalithic Site of al-Midamman, Yemen: an Interdisciplinary Approach. *J Archaeol Sci*, 29: 195-209.
- Guidelines on the X-radiography of archaeological metalwork. 2006. English Heritage.
- Junghans, S., Sangmeister, E., Schröder, M. 1968. *Kupfer und Bronze in der frühen Metallzeit Europas*. Studien zu den Anfängen der Metallurgie 2(1-3), Gebrüder Mann Verlag, Berlin.
- Junghans, S., Sangmeister, E., Schröder, M. 1974. *Kupfer und Bronze in der frühen Metallzeit Europas*. Studien zu den Anfängen der Metallurgie 2(4), Gebrüder Mann Verlag, Berlin.
- Kallithrakas-Kontos, N., Katsanos, A.A., Touratsoglu, J. 2000. Trace element analysis of Alexander the Great's silver tetradrachms minted in Macedonia. *Nucl Inst Meth B*, 171: 342-349.
- Klein, S., Hauptmann, A. 1999. Iron Age leaded tin bronzes from Khibert Edh-Dhari, Jordan. *J Archaeol Sci*, 26: 1075-1082.
- Lechtman, H. 1996. Arsenic Bronze: Dirty copper or chosen alloy? A view from the Americas. *J Field Archaeol*, 23: 477-514.
- Mabille L., Bertrand, A., Sutter, E., Fiaud, C. 2003. Mechanism of dissolution of a Cu-13Sn alloy in low aggressive conditions. *Corros Sci*, 45: 855-866.
- Melo, A., Figueiredo, E., Araújo, M.F., Senna-Martinez, J.C. 2009. Fibulae from an Iron Age Site in Portugal. *Mater Manuf Process*, 24: 955-959.
- Montero-Ruiz, I. & Perea, A. 2007. Brasses in early metallurgy of the Iberian Peninsula. In: La Niece, S., Hook, D., Craddock, P. (Eds.) *Metals and Mines: Studies in Archaeometallurgy*. Archetype Publications, London, 136-139.

- Piccardo, P., Mille, B., Robbiola, L. 2007. Tin and copper oxides in corroded archaeological bronzes. *Corrosion of metallic heritage artefacts*. Cambridge: Woodhead Publishing Limited: 239-262.
- Rehren, T., Martín-Torres, M. 2008. Naturam ars imitata: European Brassmaking between Craft and Science. *Archaeology, History & Science*: 167-188.
- Robbiola, L., Blengino, J.M., Fiaud, C. 1998. Morphology and mechanisms of formation of natural patinas on archaeological Cu-Sn alloys. *Corros Sci*, 12: 2083-2111.
- Robbiola, L., Portier, R. 2006. A global approach to the authentication of ancient bronzes based on the characterisation of the alloy–patina–environment system. *J Cult Herit*, 7: 1-12.
- Rovira, S., Montero-Ruiz, I. 2003. Natural tin-bronze alloy in Iberian Peninsula metallurgy: potentiality and reality. In: Giunlia-Mair, A., Lo Shiavo, F. (Eds.), *Le problem de l'étain à l'origine de la métallurgie*, BAR International Series 1199, British Archaeological Reports, Oxford, 15-22.
- Rovira, S. 2004. Tecnología metalúrgica y cambio cultural en la prehistoria de la Península Ibérica. *Revista de Historia*, Vol. 17: 9-40.
- Ruiz-Gálvez; M. 1998. *La Europa Atlântica en la Edad del Bronce – Un viaje a las raíces de la Europa Occidental*. Crítica (Eds.), Barcelona.
- Ruiz-Galvez, M. 2014. The Atlantic Iberia: A threshold between East and West. *Iberia. Protohistory of the far west of Europe: from Neolithic to Roman conquest*: 161-180.
- Sandu, I.G., Mircea, O., Vasilache, V., Sandu, I. 2012. Influence of archaeological environment factors in alteration processes of copper alloy artefacts. *Microsc res techniq*, 75, 1646-1652.
- Scott, D.A. 1991. *Metallography and Microstructure of Ancient and Historic Metals*. The Getty Conservation Institute & Archetype Books.
- Senna-Martinez, J.C. 2010. “Um mundo entre mundos” – O grupo Baiões/Santa Luzia, sociedade; metalurgia e relações inter-regionais. *Iberografias*, 6: 13-26.
- Silva, R.J.C., Figueiredo, E., Araújo, M.F., Pereira, F. e Fernandes, F.M.B. 2008. Microstructure interpretation of copper and bronze archaeological artefacts from Portugal, *Mater Sci Forum*, Vols. 587-588: 365-369.
- Soares, A.M.M., Valério, P., Araújo, M.F., Alves, L.C. 2004. Análise química não-destrutiva de artefactos em ouro pré e proto-históricos: alguns exemplos. *Revista Portuguesa de Arqueologia*, 7/2, 125-138.
- Soares, A.M.M., Valério, P., Silva, R.J.C. et al. 2010. Early Iron Age gold buttons from South-Western Iberian Peninsula. Identification of a gold metallurgical workshop. *Trabajos de Prehistoria*, 67/2, 501-510.
- Stillwell, C.W., Turnipseed, E.S. 1934. Mechanism of dezincification. *Ind Engi Chem*, Vol. 26, No. 7: 740-743.
- Thornton, C.P., Ehlers, C.E. 2003. Early brass in the ancient Near East. *IAMS*, 23: 3-8.
- Tylecote, R.F. 1979. The effect of soil conditions on the long-term corrosion of buried tin-bronzes and copper. *J Archaeol Sci*, 6: 345-368.
- Tylecote, R.F. 1992. *A History of Metallurgy*. The Institute of Materials, London.
- Valério, P., Araújo, M.F., Senna-Martinez, J.C., Inês Vaz, J.L. 2006. Caracterização química de produções metalúrgicas do Castro da Senhora da Guia de Baiões (Bronze Final). *O Arqueólogo Português*, 24: 289-319.

- Valério, P., Soares, A.M.M., Araújo, M.F. *et al.* 2007a. Vestígios arqueometalúrgicos do povoado calcolítico fortificado do Porto das Carretas (Mourão). *O Arqueólogo Português*, Série IV, 24: 289-319.
- Valério, P., Araújo, M.F., Canha, A. 2007b. EDXRF and Micro-EDXRF studies of Late Bronze Age metallurgical productions from Canedotes (Portugal). *Nucl Instrum Meth B*, 263: 477-482.
- Vilaça, R. 1997. Metalurgia do Bronze Final da Beira Interior: revisão dos dados à luz de novos resultados. *Estudos Pré-Históricos V*: 123-154.
- Vilaça, R. 2006. Artefactos de ferro em contextos do Bronze Final do território português: Novos contributos e reavaliação dos dados. *Complutum*, vol 17: 81-101.
- Valério, P. 2012. *Archaeometallurgical Study of Pre and Protohistoric Production Remains and Artefacts from Southern Portugal*. Tese de Doutoramento. Universidade Nova de Lisboa.
- Valério, P., Araújo, M.F., Silva, R.J.C. 2014. Complementary use of X-ray methods to study ancient production remains and metals from Northern Portugal. *X-Ray Spectrom*, 43: 209-215.
- Vilaça, R. 2006. Depósitos de Bronze do Território Português – Um debate em aberto. *O Arqueólogo Português* 24: 9-150.
- Vilaça, R. 2009. Sobre tranchets do Bronze Final do Ocidente Peninsular. *Portugalia*, XXX: 61-84.
- Wang, Q., Ottaway, B.S. 2004. *Casting experiments and microstructure of archaeologically revelant bronzes*. BAR IS 1331, Archeopress, Oxford,
- Wang, Q., Merkel, J.F. 2001. Studies on the redeposition of copper in Jin bronzes from Tianma Qucun, Shanxi, China. *Stud Conserv*, 46: 242-250.

## **Appendices**

**Appendix I. Artefacts details and particularities**

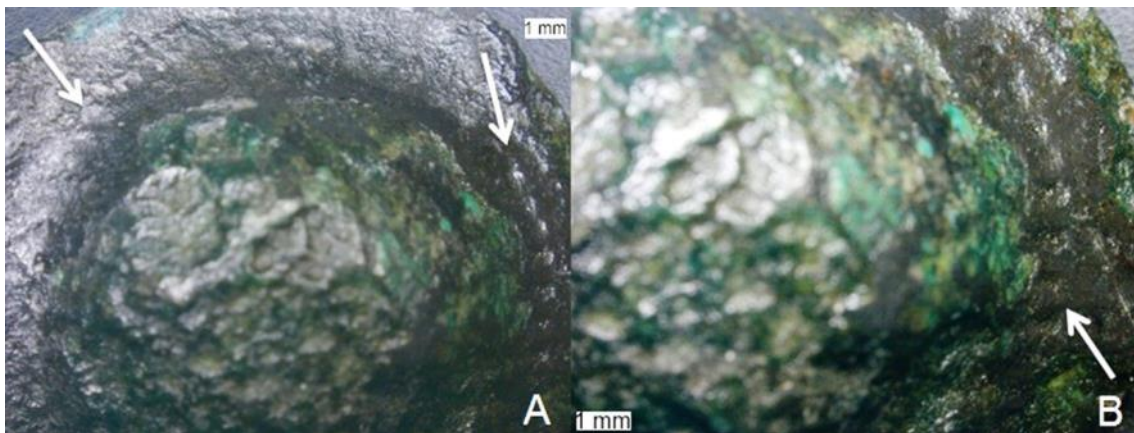


**Figure A1.** Decoration of the button 2013-0446 (A 7.5x; B 10x) under stereomicroscope.



**Figure A2.** Detail of the marks present in the nail 2013-0447 under stereomicroscope (right 10x).

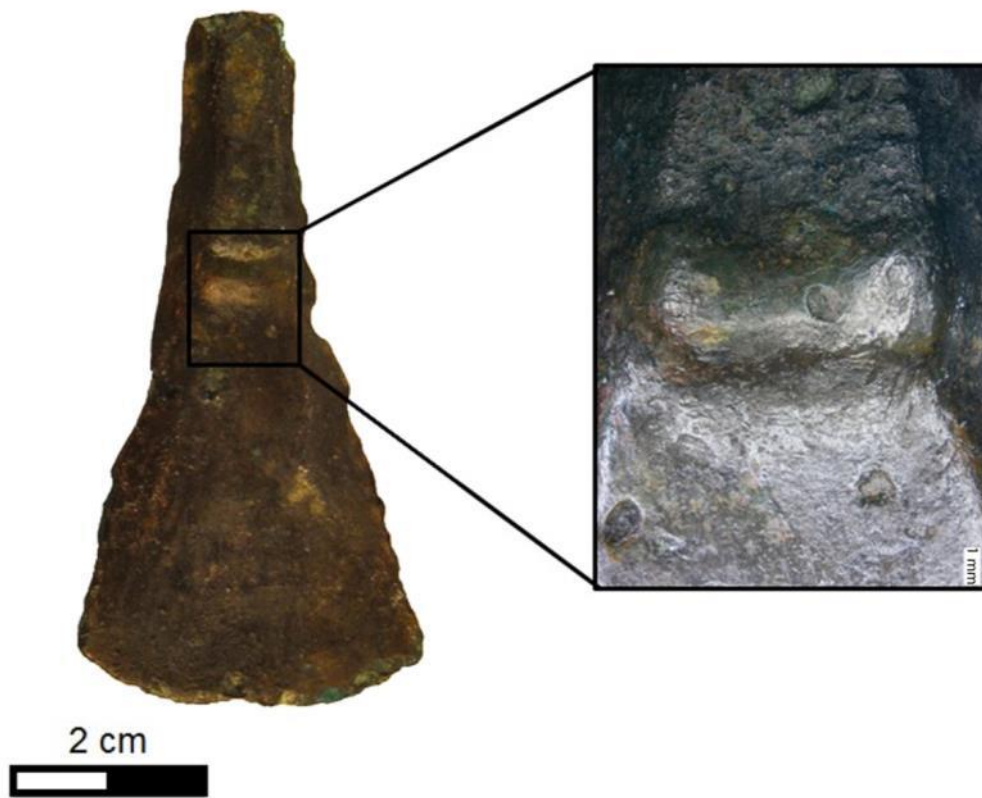


**Figure A3.** Detail of the horizontal rib of the tranchet 2013-0426 under stereomicroscope (right 10x).

Appendix II. Phase diagrams

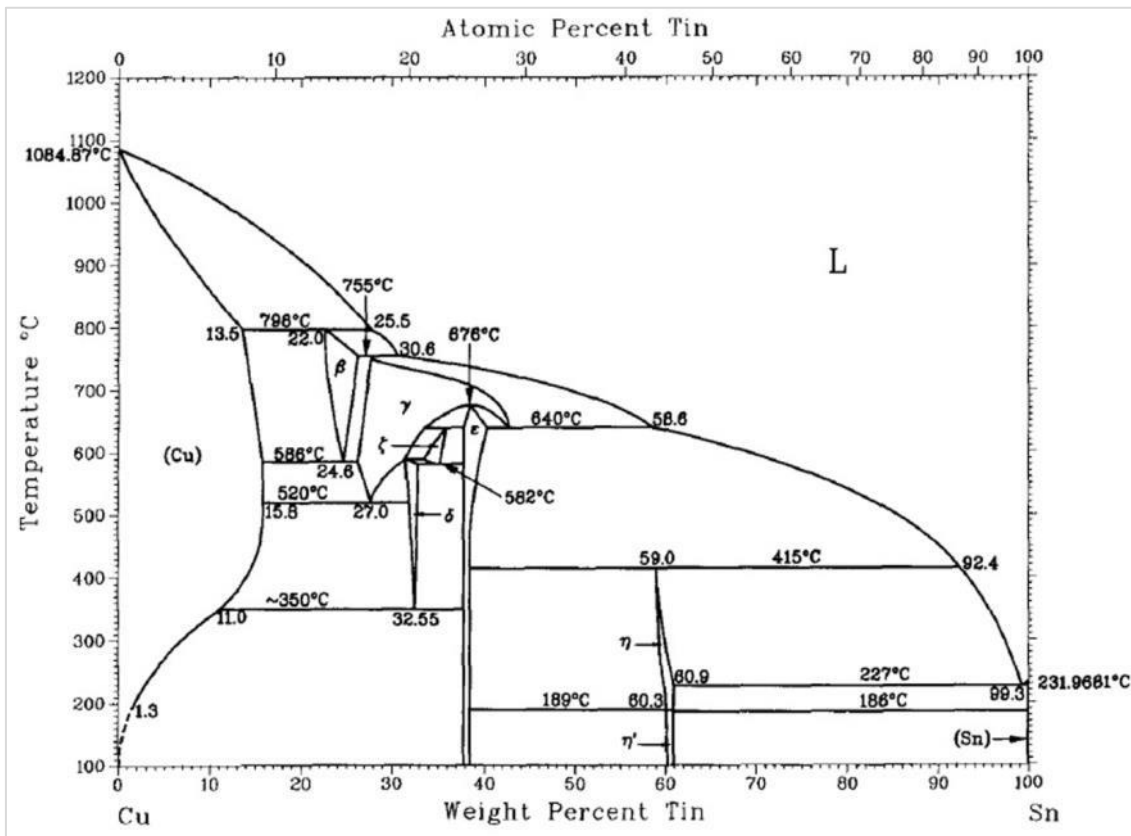


Figure A4. Copper-tin phase diagram (Bulletin of Alloy Phase Diagrams Vol. 11 No. 3 1990).

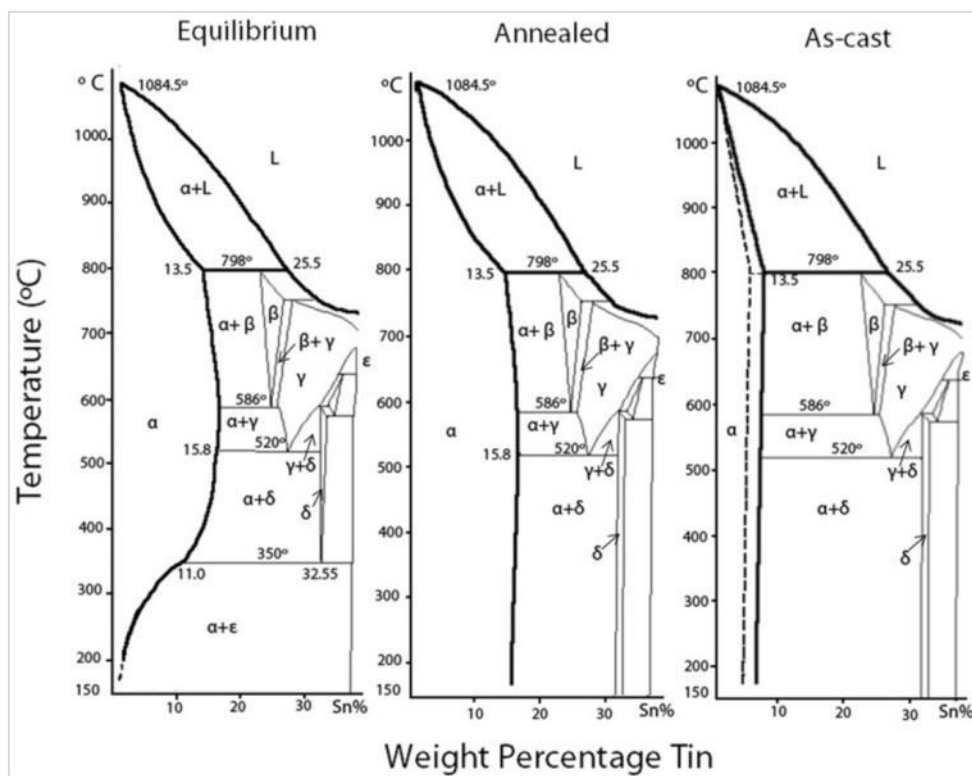
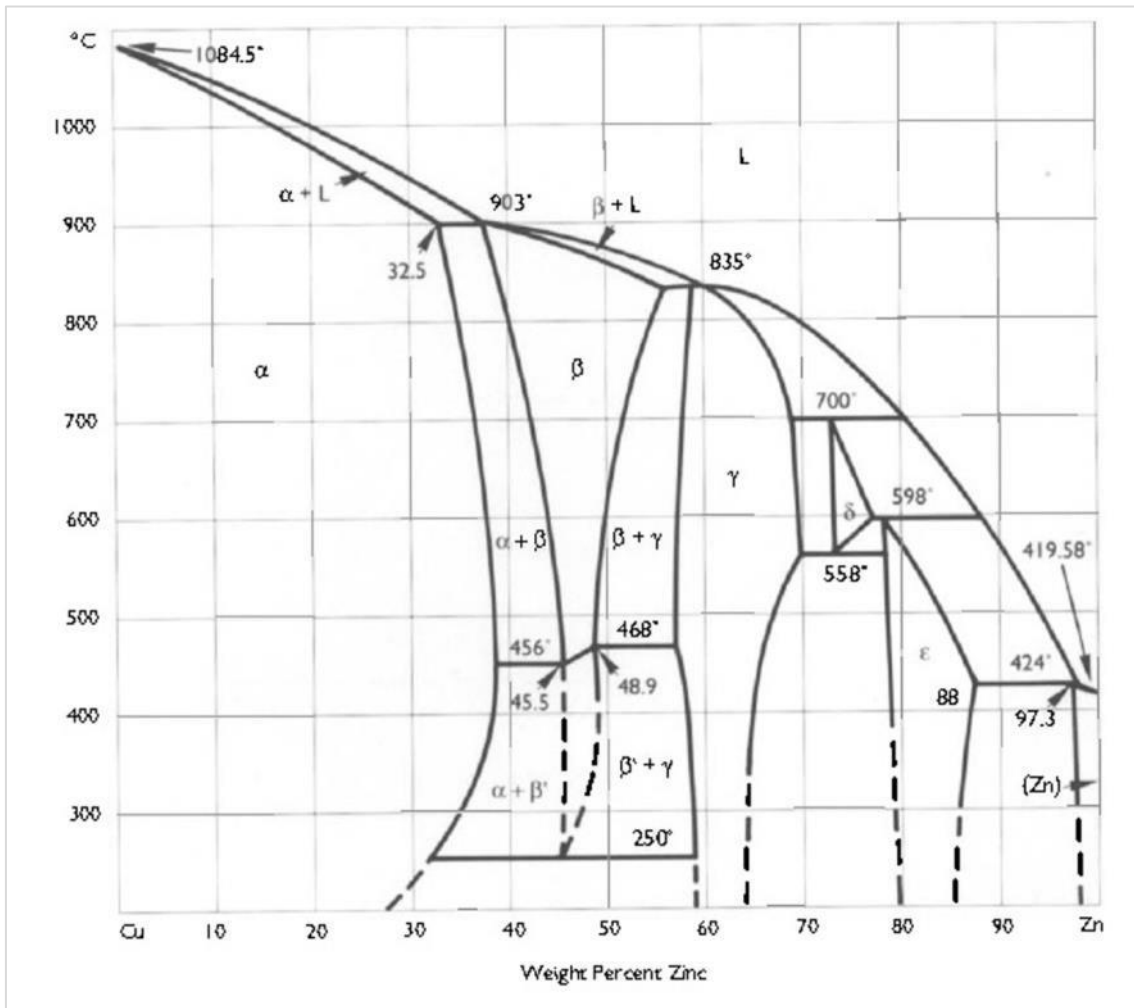


Figure A5. Equilibrium and metastable phase diagrams for Cu-Sn system based on Centre Technique des Industries des Alliages Cuivreux. 1967. *Atlas Metallographique des Alliages Cuivreux*. Paris: Éditions Techniques des Industries de la Fonderie.



**Figure A6.** Copper zinc phase diagram (Scott, David A. 1991. *Metallography and Microstructure of Ancient and Historic Metals*. The Getty Conservation Institute & Archetype Books).

### Appendix III. Microstructural characterisation of MG artefacts

**Table A1.** OM characterization of the copper-based artefacts (\*: % given by micro-EDXRF; +: Influence of corrosion; C: Casting; D: Deformation/forging; T: heat treatment/annealed; ↓ low amount; ↑ high amount; other: other small dark inclusion, possibly Cu-S-Fe in bronzes and Sn-O in coppers).

| Reference | Typology | Sn wt. % * | Phases    | Manufacture                 | Inclusions |        |
|-----------|----------|------------|-----------|-----------------------------|------------|--------|
| 2013-0423 | Dagger   | Blade      | 12.8±1.2  | $\alpha + \delta$           | C+T        | S      |
|           |          | Center     | 29.9±1.96 | $\alpha + \delta$           | C          | S      |
|           |          | Top        | 18.8±4.4  | $\alpha + \downarrow\delta$ | C+D+T+D    | S      |
| 2013-0424 | Dagger   | Blade      | 13.7±0.9  | $\alpha$                    | C+D+T      | S      |
|           |          | Center     | 12.2±1.0  | $\alpha + \delta$           | C+D+T+↓D   | S      |
|           |          | Top        | 13.3±0.5  | $\alpha + \delta$           | C+D+T+↑D   | S      |
| 2013-0425 | Dagger   |            | 15.3±1.1  | $\alpha$                    | C+D+T+↑D   | S      |
| 2013-0426 | Tranchet | Blade      | 19.1±3.41 | $\alpha + \uparrow\delta$   | C+D+T      | ↑ S    |
|           |          | p1         | 14.9±0.3  | $\alpha + \uparrow\delta$   | C+D        | ↑ S    |
|           |          | p2         | 15.5±0.5  | $\alpha + \uparrow\delta$   | C+D+T      | ↑ S    |
|           |          | Top        | 14.7±0.3  | $\alpha + \uparrow\delta$   | C+D+T      | ↑ S    |
| 2013-0427 | Bar      |            | 13.8±0.3  | $\alpha + \delta$           | C+D+T      | ↑ S    |
| 2013-0428 | Wire     |            | n.d.      | $\alpha$                    | C+↓D+T+↓D  | S, ds  |
|           | Ring 01  |            | 13.2±0.3  | $\alpha + \delta$           | C+D+T      |        |
|           | Ring 02  |            | 13.5±0.1  | $\alpha + \uparrow\delta$   | C+D+T      |        |
| 2013-0429 | Ring     |            | 12.7±0.2  | $\alpha + \delta$           | C+D+T+D    | S, ds  |
| 2013-0430 | Ring     |            | 11.8±0.6  | $\alpha + \delta$           | C+D+T+D    | S, ds  |
| 2013-0431 | Ring     |            | 13.0±0.1  | $\alpha + \delta$           | C+↓D+T     | S, ds  |
| 2013-0434 | Ring     |            | 1.3±0.6   | $\alpha$                    | C+D+↓T     | S, ds? |
| 2013-0435 | Ring     |            | 1.2±0.3   | $\alpha$                    | C+↓T       | S, ds  |
| 2013-0436 | Ring     |            | 12.0±1.2  | $\alpha$                    | C+D+T+D    | S, ds  |
| 2013-0437 | Ring     |            | n.d.      | $\alpha$                    | C+D+↓T     | S      |
| 2013-0438 | Ring     |            | 14.6±0.9  | $\alpha + \delta$           | C+D+T+↑D   | S      |
| 2013-0439 | Ring     |            | 13.8±0.5  | $\alpha + \uparrow\delta$   | C+D+T      | S, ds  |
| 2013-0440 | Ring     |            | 14.5±0.6  | $\alpha$                    | C+↓D       | S      |
| 2013-0441 | Ring     |            | 2.9±0.1   | $\alpha + \delta$           | C+↓D       | S      |
| 2013-0442 | Ring     |            | 3.5±0.5   | $\alpha, \delta?$           | C          | S      |
| 2013-0443 | Ring     |            | 10.6±1.5  | $\alpha + \downarrow\delta$ | C+↓T       | ↓ S    |
| 2013-0444 | Ring     |            | 13.6±0.95 | $\alpha + \uparrow\delta$   | C+↓D       | S      |
| 2013-0445 | Ring     |            | 8.1±0.8   | $\alpha$                    | C+↑D       | S, ds? |
| 2013-0446 | Button   | Side       | 14.0±0.2  | $\alpha$                    | C+↓D+T     | S, ds? |
|           |          | Interior   | 12.0±0.7  | $\alpha$                    | C+↓D+T     | S, ds? |
| 2013-0447 | Nail     | Head       | 12.0±1.1  | $\alpha$                    | C+D+T      | S      |
|           |          | Pin        | 10.0±0.5  | $\alpha$                    | C+D+T+↑D   | S, ds  |
| 2013-0448 | Pendant  | Head       | 13.2±0.1  | $\alpha + \delta$           | C+D        | S, ds  |
|           |          | Pin        | 13.3±0.2  | $\alpha + \delta$           | C+D+↑T+D   |        |
| 2013-0449 | Pendant  | Head       | 12.3±1.5  | $\alpha + \delta$           | C          | S, ds  |
|           |          | Pin        | 12.6±0.2  | $\alpha$                    | C+↓D       | S, ds? |
| 2013-0450 | Bar      |            | 13.0±1.1  | $\alpha$                    | C+↓D+T+↓D  | S, ds  |
| 2013-0451 | Bar      |            | 12.0±0.8  | $\alpha$                    | C+D+T+↓D   | S, ds  |
| 2013-0452 | Bar      |            | 11.9±0.7  | $\alpha + \downarrow\delta$ | C+↓D+T+↓D  | ↓S, ds |
| 2013-0453 | Bar      |            | 1.3±0.3   | $\alpha$                    | C+↓D+T+↓D  | S, ds  |
| 2013-0454 | Bar      |            | 4.9±0.9   | $\alpha$                    | C+↓D+T+↓D  | S, ds  |
| 2013-0455 | Bar      |            | 12.1±0.8  | $\alpha + \delta$           | C+↑D       |        |
| 2013-0456 | Sheet    |            | n.d.      | $\alpha$                    | C+D+T      | S?     |
| 2013-0457 | Capsule  |            | n.d.      |                             | C+D+T      |        |

## Appendix IV. Microstructures of the artefacts

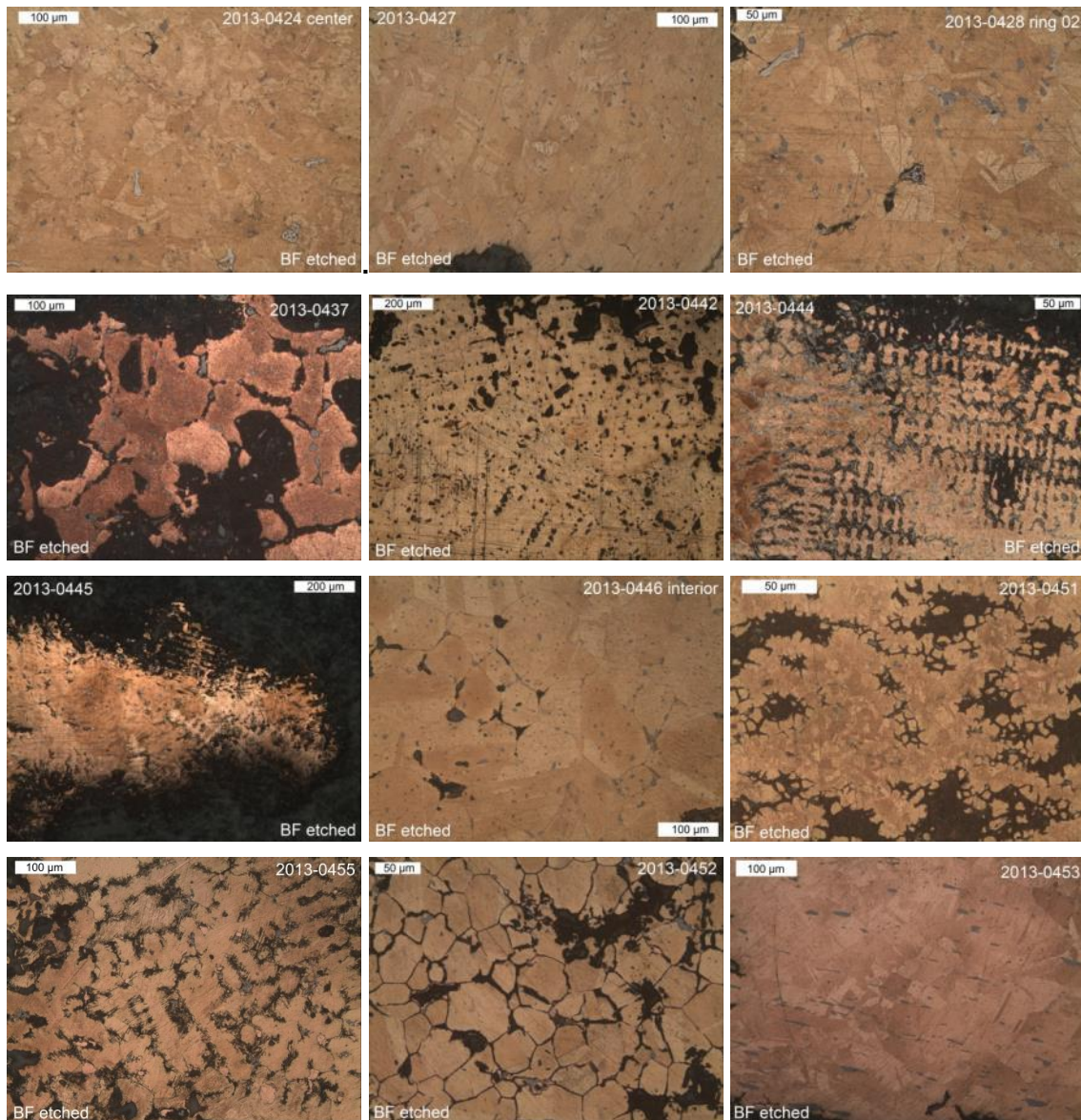


**Figure A7.** Microstructures of some of the MG collection artefacts.

## Appendix V. SEM-EDS analyses

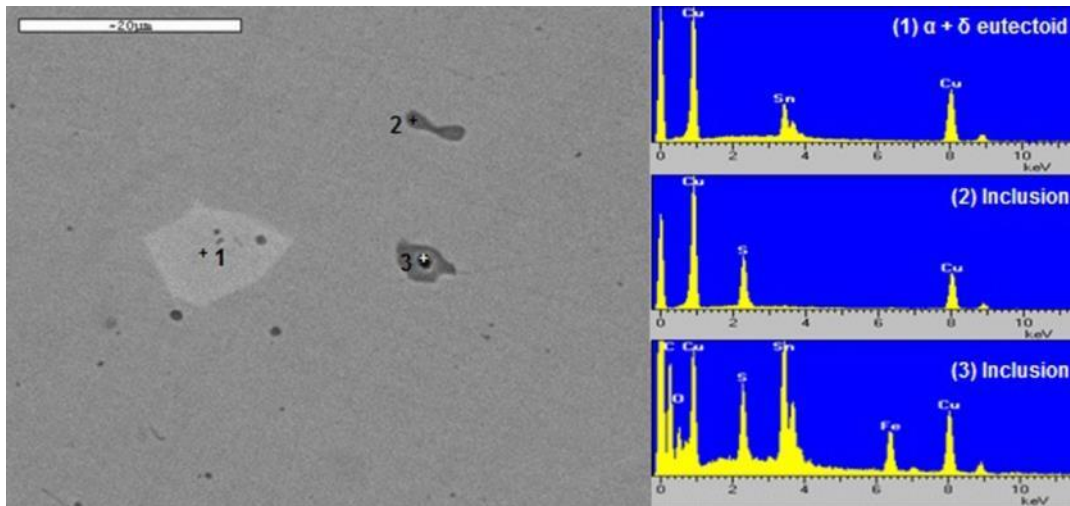


**Figure A8.** SEM (BE) image and spot EDS analysis of the (1)  $\alpha + \delta$  eutectoid, (2) Cu-S inclusion and (3) Cu-S-Fe inclusion on the bronze ring 2013-0431.

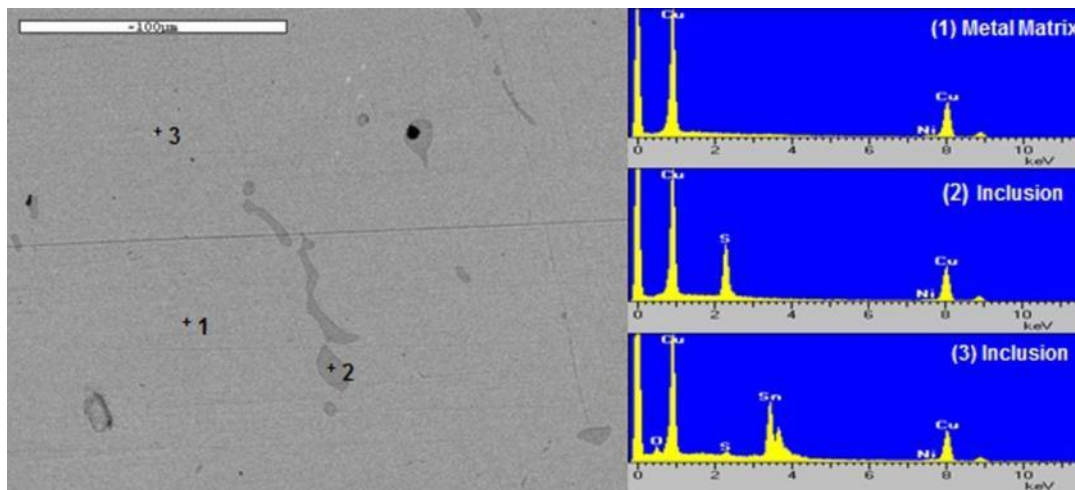


**Figure A9.** SEM (BE) image and spot EDS analysis of the (1) Metal matrix, (2) Cu-S inclusion and Ni and (3) Sn-O inclusion on the copper ring 2013-0435.

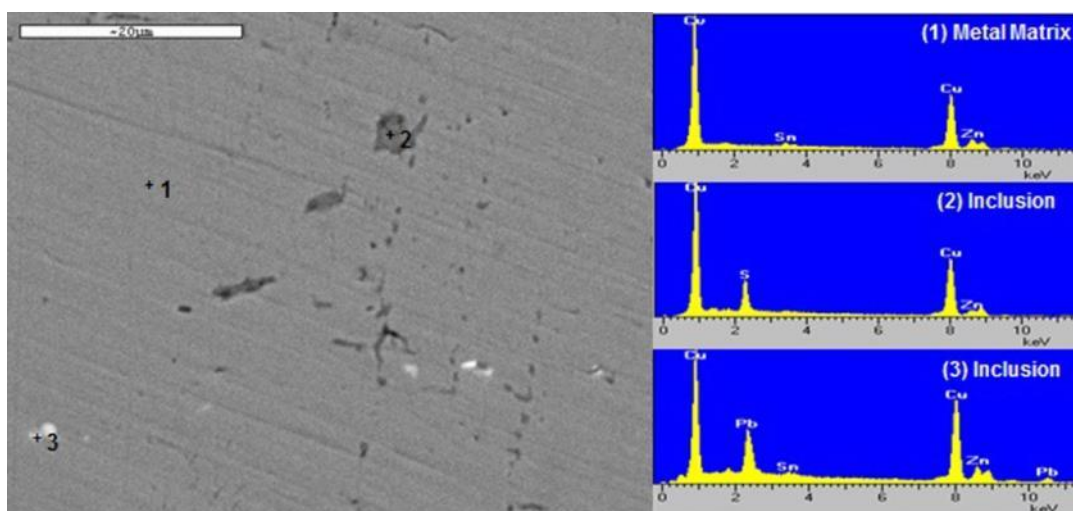


**Figure A10.** SEM (BE) image and spot EDS analysis of the (1) Metal matrix, (2) Zn-S inclusion and (3) Pb inclusion on the brass ring 2013-0441.

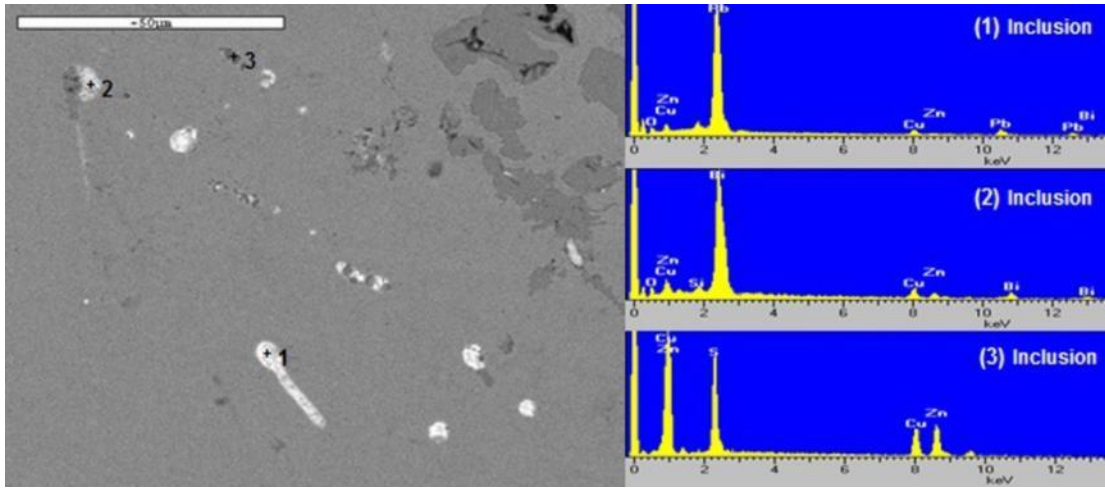


**Figure A11.** SEM (BE) image and spot EDS analysis of the (1) Pb inclusion with some Bi, (2) Bi inclusion and (3) Zn-S inclusion on the capsule 2013-0457.